# Divergent ion selectivity and sensitivity to anti-hypertensive and non-steroidal anti-inflammatory drugs of DEG/ENaC/ASIC channels in *C. elegans*

Fechner, S.[1], D'Alessandro, I.[1], Wang, L.[1], Tower, C.[1], Tao, L.[2], *Goodman, M.B.[1]

[1]Department of Molecular and Cellular Physiology, Stanford University, School of Medicine, Stanford, CA, 94305

[2]Department of Biology, Stanford University, CA, 94305

*Correspondence to: mbgoodman@stanford.edu

**Abstract**

The degenerin channels, epithelial sodium channels, and acid-sensing ion channels (DEG/ENaC/ASICs) play important roles in sensing mechanical stimuli, regulating salt homeostasis, and responding to acidification in the nervous system. They share a common topology with two transmembrane domains separated by a large extracellular domain and are believed to assemble as homomeric or heteromeric trimers into non-voltage gated, sodium-selective, and amiloride-sensitive ion channels. Amiloride is not the only drug that targets DEG/ENaC/ASICs, however; they are also emerging as a target of nonsteroidal anti-inflammatory drugs (NSAIDs). *C. elegans* has about 30 genes encoding DEG/ENaC/ASIC subunits and thus offers an excellent opportunity to examine variations in the biophysical properties and sensitivity to small molecules of these subunits. Here, we analyzed a subset of the *C. elegans* DEG/ENaC/ASIC proteins in order to test the hypothesis that individual family members have distinct properties. Toward this goal, we expressed five *C. elegans* isoforms in *Xenopus laevis* oocytes (DEGT-1d, DEL-1d, UNC-8d, MEC-10d and MEC-4d) and measured current amplitude, selectivity among monovalent cations, sensitivity to amiloride and its analogs, and sensitivity to NSAIDs. Of these five proteins, only DEGT-1d, UNC-8d, and MEC-4d form homomeric channels. Unlike MEC-4d and UNC-8d, DEGT-1d channels were insensitive to amiloride and its analogs and more permeable to $K^+$ than to $Na^+$. As reported for rat ASIC1a, NSAIDs inhibit DEGT-1d and UNC-8d. Unexpectedly, MEC-4d was strongly potentiated by NSAIDs, an effect that was decreased by mutations in the extracellular domain that affect inhibition of rat ASIC1a. Collectively, these findings reveal that not all DEG/ENaC/ASIC channels are amiloride-sensitive and sodium-selective and that NSAIDs can both inhibit and potentiate these channels.

## Introduction

The degenerin channels, epithelial sodium channels, and acid-sensing ion channels (DEG/ENaC/ASICs) are present in most, if not all metazoans and expressed in diverse tissues, including the epithelia of several organs and in the central and peripheral nervous systems (Eastwood and Goodman, 2012; Kellenberger and Schild, 2002). These channels vary in how they are activated *in* vivo, although the activation mechanisms are not yet known for all family members. At least two DEG proteins are known to be mechanosensitive, ENaCs are constitutively active and can be regulated by shear stress, and ASICs are activated by proton binding (Eastwood and Goodman, 2012). The DEG and ENaC proteins were the initial members of this superfamily. The DEGs were identified in *C. elegans* by virtue of their role in mechanosensation and neuronal degeneration (Chalfie and Wolinsky, 1990; Driscoll and Chalfie, 1991; Huang and Chalfie, 1994). The ENaCs were identified *via* expression of rodent cRNAs in Xenopus oocytes followed by functional screening (Canessa et al., 1995). The proteins that form acid-sensing ion channels (ASICs) were also identified in the 1990s (Waldmann et al., 1997) and are homologous to Degenerins and ENaCs (García-Añoveros et al., 1997; Kellenberger and Schild, 2002).

All of these proteins have two transmembrane domains linked by a large extracellular domain which is divided into structures described by a hand holding a ball: wrist, finger, ball, and knuckle. This view has emerged from high-resolution structures derived from x-ray diffraction of protein crystals (Baconguis et al., 2014; Dawson et al., 2012; Gonzales et al., 2009; Jasti et al., 2007; Noreng et al., 2018) and cryo-electron microscopy of chicken ASIC1a (Sun et al., 2018; Yoder et al., 2018). Individual proteins assemble into trimers and form a pore along a common three-fold access at the center of the complex. The extracellular finger domain exhibits more sequence variation than other domains and the general topology of all family members are assumed to share the same fold as ASIC1a. Although ENaCs are formed from three distinct proteins, many DEGs and ASICs form both homomeric and heteromeric channels. Thus, the ensemble of functional channels is expanded not only by genetic variation of individual channel subunits, but also by the formation of DEG and ASIC heteromeric channels.

The ENaC channels are crucial for salt homeostasis and are blocked by amiloride [reviewed by (Garty and Benos, 1988; Palmer, 1992)], a classical anti-hypertension drug that functions as an open-channel blocker (Schild et al., 1997). Sensitivity to amiloride and its

analogs is not limited to mammalian family members or to ENaCs, however, but is also seen in DEG/ENaC/ASIC channels expressed in invertebrates. Amiloride is a potent (sub-micomolar $IC_{50}$) blocker of DEG and ENaC channels, but is at least hundred-fold less potent as a blocker of ASIC channels (Canessa et al., 1994; Goodman et al., 2002; Vullo and Kellenberger, 2019). Despite widespread findings of amiloride as an inhibitor, amiloride potentiates the activity of at least two DEG/ENaC/ASIC channels (Adams et al., 1999; Elkhatib et al., 2019). It is not known whether amiloride potentiation and inhibit arise from binding to distinct or similar sites within channels. Among channels inhibited by amiloride, variations in sensitivity could reflect differences in binding affinity or in the efficacy of inhibition. It remains unknown if sensitivity to amiloride or its analogs is a universal feature of DEG/ENaC/ASIC channels.

The ASIC channels are implicated in neurological disease and in pain sensation, but there are no potent and selective small molecule inhibitors of ASICs available (Boscardin et al., 2016; Hanukoglu and Hanukoglu, 2016; Kellenberger and Schild, 2015; Vullo and Kellenberger, 2019). Evidence is emerging that ASICs are targets of non-steroidal anti-inflammatory drugs (NSAIDs). In particular, ibuprofen is an effective (micromolar $IC_{50}$) allosteric inhibitor of $H^+$-evoked ASIC1a currents and mutations in the wrist and the first transmembrane domain (TM1) reduce the apparent affinity for ibuprofen (Lynagh et al., 2017b). This finding implicates NSAIDs as an additional class of small molecules affecting the function of DEG/ENaC/ASIC channels, providing an additional tool for biophysical and functional studies.

Whereas mammalian genomes have nine genes encoding ENaC and ASIC proteins (Hanukoglu and Hanukoglu, 2016; Kellenberger and Schild, 2002), the *C. elegans* genome harbors more than two dozen genes encoding DEG/ENaC/ASIC proteins (Goodman and Schwarz, 2003; Hobert, 2013). The extracellular finger domains are the most variable domains among the *C. elegans* family members and between families that have undergone expansion in different animal genomes (Eastwood and Goodman, 2012; Hanukoglu and Hanukoglu, 2016). Thus, the *C. elegans* set of DEG/ENaC/ASIC proteins offers an excellent opportunity to examine variations in the biophysical properties within this superfamily. As an entry point for exploration, we expressed five DEG/ENaC/ASIC proteins in *Xenopus* oocytes individually and tested their ability to form functional channels, measured their permeability to monovalent cations, and examined their response to amiloride and its analogs as well as a set of NSAIDs. The five DEG/ENaC/ASIC proteins we studied, DEGT-1d, DEL-1d, UNC-8d, MEC-10d and MEC-4d,

are known to be expressed in touch receptor neurons [MEC-4, MEC-10, and DEGT-1 (M Chatzigeorgiou et al., 2010; Driscoll and Chalfie, 1991; Huang and Chalfie, 1994)] or in mechanical nociceptors [UNC-8, MEC-10, DEL-1 (Marios Chatzigeorgiou et al., 2010; Tavernarakis et al., 1997)] where they are either known or proposed to contribute to the formation of mechanosensitive ion channels. We engineered these channels to be constitutively active based upon reported gain-of-function mutations that cause necrotic cell death – the "d" isoform. We found that DEGT-1d forms a homomeric channel that is insensitive to amiloride and its analogs, equally permeable to $K^+$ than to $Na^+$, and blocked by NSAIDs. Consistent with prior studies, the expression of MEC-10d (Goodman et al., 2002) or DEL-1d was not sufficient to generate any detectable ionic current and both MEC-4d and UNC-8d formed channels that were $Na^+$-selective and blocked by amiloride (Goodman et al., 2002; Wang et al., 2013). Unexpectedly, MEC-4d-dependent current was strongly potentiated by NSAIDs and sensitivity to these drugs was decreased by mutations in the extracellular domain that affect inhibition of rat ASIC1a by ibuprofen, a frontline NSAID drug. Collectively, these findings reveal that not all DEG/ENaC/ASIC channels are amiloride-sensitive and sodium-selective and that NSAIDs can both potentiate and inhibit these channels.

## Methods

*Expression constructs and molecular biology*

Plasmids carrying native cDNAs encoding MEC-4, MEC-10 and other *C. elegans* DEG/ENaC/ASIC proteins derived from the *C. elegans* genome are subject to deletions and recombination when propagated in standard bacterial strains (Chalfie et al., 2003; Goodman et al., 2002). Previously, we circumvented this outcome using a bacterial strain, SMC4, specifically derived for this purpose (Chalfie et al., 2003; Goodman et al., 2002) Here, we used an alternative strategy that enables us to propagate expression plasmids in standard bacterial strains (NEB 5-alpha Competent *E. coli*, High Efficiency): synthetic cDNAs codon-optimized for expression in insect cells. Accordingly, we obtained plasmids containing synthesized codon-optimized cDNAs encoding full-length MEC-4, MEC-10 and DEGT-1 (GenScript) in the pGEM-HE oocyte expression vector (Liman et al., 1992). DEL-1 was codon-optimized for expression in *C. elegans* (IDT) based on the predicted sequence reported in wormbase release WS250. The predicted

isoforms encoded by the *del-1* locus have been modified in a more recent database releases (WS274) and these changes are evident only in the amino terminal domains. WS274 predicts three isoforms and the isoform we used from WS250 encodes 18 amino acids that are not represented in the updated predictions. Unlike MEC-4, MEC-10, DEL-1 and DEGT-1, the UNC-8 isoform was not codon-optimized. This plasmid was obtained from L. Bianchi, used in several prior studies (Matthewman et al., 2018, 2016; Miller-Fleming et al., 2016; Wang et al., 2013), and encodes the shortest of four predicted splice variants (R13A1.4d).

We studied the expressed channels as constitutively-active or degeneration ('d') isoforms based on gain-of-function mutations identified in forward genetic screens or engineered into homologous residues. Because co-expressing MEC-2 yields larger currents than expressing MEC-4d alone and co-expressing MEC-2 with UNC-8d is either indifferent or may yield to larger currents than expressing UNC-8d alone (Brown et al., 2007; Goodman et al., 2002; Matthewman et al., 2016), we co-expressed MEC-2 with all DEG/ENaC/ASIC channels studied here.

We used *in vitro* mutagenesis (Q-5 Site-directed Mutagenesis Kit, NEB) to introduce the mutations creating *d* isoforms using the following primers. All mutations were introduced into plasmids encoding wild-type protein, except the last two mutant isoforms that introduced second mutations into plasmids encoding MEC-4[A713T].

MEC-4[A713T]:
CTCTTGACTGACTTCGGTGG, GTTCACGAAACCGTAGGCTT;

MEC-10[A676V]:
AAGATGATGGTTGACTTCGGC, CACGATACCGTAGGCCTC

DEGT-1[A813T]:
CTCTTGACTGAGATCGGAGG, CAGGAACAAGTTGTAGGAGC.

UNC-8[G347E]:
AAAGATGCGGAAGCCATCACA, GAGGTCGCTCAATCCAAAAG

DEL-1[A603V]:

AATTTGATGGTCGATATGGGAG, GAACCATGAATATGACTCG

MEC-4[A713T, E704K]:
CTCTTGACTGACTTCGGTGG, GTTCACGAAACCGTAGGCTT (A713T);
GGCCTACGGTTTCGTGAACCTCT, TTGGACTCGGTGAGCATCTCGAA (E704K)

MEC-4[A713T,E704A]:
CTCTTGACTGACTTCGGTGG, GTTCACGAAACCGTAGGCTT (A713T);
GCGGACTCGGTGAGCATCTC, AGCCTACGGTTTCGTGAACCTC (E704A)

*RNA preparation, validation and oocyte injection*

For each channel isoform, we generated capped RNAs (cRNA) using *in vitro* transcription (mMESSAGE mMACHINE T7 kit, Ambion) and quantified cRNA concentration spectroscopically (NanoDrop2000, Thermo Fisher Scientific). We validated the size and integrity of cRNAs using gel electrophoresis and pre-cast RNA gels (Reliant®RNA Gels, 1.25% SKG, Lonza). To each cRNA sample, we added buffer (2 µL 10x MOPS buffer, Lonza) and loading dye (8 µL, B0363S, NEB) and loaded denatured (70 °C, 10 minutes) samples alongside an RNA ladder (2-4 µL, ssRNA ladder, N0362S, NEB). The resulting gels were stained with ethidium bromide for 30 minutes (0.5 µg/mL $ddH_20$, Thermo Fisher Scientific), washed in $ddH_20$ (30 minutes), and visualized with UV light.

*Xenopus laevis* oocytes were isolated from gravid females (NASCO) modified from standard procedures (Liu and Liu, 2006). Briefly, frogs were anesthetized with MS-222 (0.5%, 1hr), follicles were removed, opened with forceps and transferred to OR-2 solution. For defolliculation, oocytes were incubated twice (1st 45 min, 2nd variable) in OR-2 containing 3 mg/ml collagenase type IV (Sigma, C-9891). Defolliculated oocytes were stored in ND96 solution containing (in mM): NaCl 96, KCl 2.5, $MgCl_2$ 1, $CaCl_2$ 1.8, Hepes 5 at pH 7.6, adjusted with NaOH, containing 10 mg/ml Penicillin-streptomycin solution (Sigma, P0781). The OR-2 solution contained (in mM): NaCl 82.5, KCl 2.5, $MgCl_2$ 1, Hepes 5 at pH 7.6. We injected cRNA encoding a single DEG/ENaC/ASIC isoform (5 ng) and MEC-2 cRNA (15 ng) in each oocyte. We reduced cRNA amounts to 3 ng (MEC-4d isoforms) and 9 ng (MEC-2) for cells used to collect ibuprofen dose-response curves. We maintained oocytes at 18°C in modified Leibovitz

medium (L-15) (Sigma Aldrich) supplemented with gentamicin (144 μM) (Gibco) and amiloride (300 μM) for 2–9 days, as described (Brown et al., 2007). Oocytes expressing UNC-8d were maintained in the same solution with additional 100 μM benzamil. To minimize the impact of variation in expression efficiency and endogenous ion channels, we report data from oocytes derived from at least three donor frogs for each channel isoform.

*Whole-cell recordings and external solutions*

Membrane current was measured by two-electrode voltage clamp (TEVC; OC-725C, Warner Instruments, LLC) at room temperature (21–24°C). Electrodes (~0.3 MΩ) were fabricated from borosilicate glass (G100TF-4, Warner Instruments, LLC) on a horizontal puller (P-97; Sutter Instruments) and filled with 3 M KCl. Analogue signals (current, voltage) were digitized (Instrutech, ITC-16), filtered at 200 Hz (8-pole Bessel filter), and sampled at 1 kHz. A 60-Hz notch filter (FLA-01, Cygnus Technology, Inc.) was used to reduce line noise. This equipment was controlled by Patchmaster software (HEKA) on a windows PC.

Unless otherwise indicated, oocytes were superfused with control saline containing (in mM) Na-gluconate (100), KCl (2), $MgCl_2$ (2), $CaCl_2$ (1) and HEPES (10), adjusted to pH 7.4 with NaOH. Drugs were diluted from stock solutions and added to control saline. To measure relative permeability ratios (Px/PNa), we omitted the 2 mM KCl in the control saline solution and replaced Na-gluconate (100) with K-gluconate (100), NMG-gluconate (100), Cs-gluconate (100) and Li-gluconate (100), adjusted to pH 7.4 with gluconate. For pH 6.4 and 8.4 solution, we replaced HEPES in the control saline with 10 mM PIPES and 10 mM TAPS, respectively.

We purchased putative antagonists and agonists from the indicated suppliers and established stock solutions in DMSO. We used stock solutions of 0.1 M, except for phenamil (0.01M) and when we were using ibuprofen and aspirin in the dose-response experiments (0.24 M). Drugs were obtained from these suppliers: amiloride (Sigma-Aldrich, A7410), benzamil (Sigma-Aldrich, B2417), 5-(N-Ethyl-N-isopropyl)amiloride (Sigma-Aldrich, A3085), phenamil (Cayman Chemical, 14308), benzamidine (Fluka, 12072), ibuprofen (Sigma-Aldrich, SLBR3566V), R-ibuprofen (Cayman Chemical, 16794), S-ibuprofen (Cayman Chemical, 375160), aspirin (Sigma-Aldrich, A2093), salicylic acid (Sigma-Aldrich, S5922), diclofenac (Sigma-Aldrich, D6899), flurbiprofen (Sigma-Aldrich, F8514).

*Measuring current, drug sensitivity, and reversal potentials*

We used two voltage protocols to measure membrane current and its response to amiloride analogs and NSAIDs: a voltage ramp (from -100 to +100 mV in 1 s) and voltage steps (from -100 to +40 mV or +60 mV, in 20 mV increments). Both protocols included a conditioning step to -85 mV, which we used to measure current amplitude. In all cases, the holding potential was -60 mV. We applied these protocols repetitively during the application of drugs and solutions with modified ion composition; the ramp protocol to measure reversal potentials.

To measure the change in current upon drug application (referred as Drug mediated current ΔI (μA)), the step and ramp protocol (Fig. 1A) was applied repetitively and the mean current at -85 mV (200 ms step) in different solutions was averaged over the last three step and ramp repetitions. We display the comparison of a drug-mediated current compared to drug-mediated current in uninjected oocytes and refer to it as ΔI baseline corrected (μA). A voltage ramp (from −100 to +100 mV in 1 s) was applied after a 100 ms step to -100 mV and reversal potentials calculated for different solutions. To calculate drug sensitivity at different voltages and reversal potentials to calculate relative permeabilities, we applied a similar voltage protocol with voltage steps from -100 to +40 or +60 mV in 20 mV increment steps. In both cases, three replicates of the voltage step protocol were averaged.

To calculate permeability ratios, $P_x/P_{Na}$, we measured reversal potentials derived from voltage steps in solutions containing different monovalent cations and used the following equation to obtain a value for $P_x/P_{Na}$: $(E_{rev}^{X+}-E_{rev}^{Na+}) = RT/zF \ln P_x[X^+]_o/P_{Na}$, with $RT/zF = 25.6$ at room temperature. This bi-ionic permeability equation (Hille, 2001) is simplified to: $P_x/P_{Na} = 1/\exp[(E_{rev}^{X+}-E_{rev}^{Na+})*1000/25.6*-1]$.

*Data Analysis & Figures:*

Mean values and reversal potentials were calculated using MATLAB (R2014b) (https://github.com/wormsenseLab/AnalysisFunction.git). ANOVA (two-way) followed by multiple comparison with the Holm-Sidak method ($P< 0.05$) was performed in Sigma Plot 12.5. Estimation statistics were performed in Python using DABEST, which is a package for Data Analysis using Bootstrap-Coupled ESTimation (Ho et al., 2019). Individual dose response curves were fitted with the Hill equation, with a Hill coefficient set to one, to calculate the

$EC_{50} = I_{max} * [x^n/(EC_{50}{}^n + x^n)]$ and $IC_{50} = I_{max} * IC_{50}{}^n/(IC_{50}{}^n + x^n)$ using IgorPro 6.37. We used the mean values for $EC_{50}$ and $IC_{50}$ to compute an average fit to the pooled and averaged data. Confidence intervals for mean relative permeability ratios were calculated in Python with DescrStatsW. Figures were prepared in python jupyter notebooks (https://github.com/wormsenseLab/JupyterNotebooksDEGENaCPharm.git).

Sequence analysis:

The following ion channel sequences were used for the phylogenetic tree: ACD-1 (C24G7.2), ACD-2 (C24G7.4), ACD-3b (C27C12.5b), ACD-4 (F28A12.1), ACD-5 (T28F2.7), ASIC-1 (ZK770.1), ASIC-2 (T28F4.2), DEG-1 (C47C12.6.1), DEGT-1 (F25D1.4), DEL-1 (E02H4.1), DEL-2a (F58G6.6a), DEL-3 (F26A3.6), DEL-4 (T28B8.5), DEL-5 (F59F3.4), DEL-6 (T21C9.3), DEL-7 (C46A5.2), DEL-8 (C11E4.3), DEL-9 (C18B2.6), DEL-10 (T28D9.7), DELM-1 (F23B2.3), DELM-2 (C24G7.1), EGAS-1 (Y69H2.11), EGAS-2 (Y69H2.12), EGAS-3 (Y69H2.2), EGAS-4 (F55G1.13), FLR-1 (F02D10.5), MEC-4 (T01C8.7), MEC-10 (F16F9.5), UNC-8d (R13A1.4d), UNC-105e (C41C4.5e), rASIC-1 (NP_077068), rASIC-2 (Q62962.1), rASIC-3 (NP_775158.1), rASIC-4 (Q9JHS6.1), rαENaC (NP_113736.1), rβENaC (NP_036780.1), rγENaC (NP_058742.2), hδENaC (001123885.2). The alignment for the calculation of the phylogentic tree was generated using MUSCL and http://www.phylogeny.fr/ (Dereeper et al., 2010, 2008) and visualized with figtree v1.4.4 (Rambaud, 2018). The alignment in Fig. 6E was generated with Clustal Omega.

**Results**

Using heterologous expression in Xenopus oocytes, we determined whether five of the more than two dozen *C. elegans* DEG/ENaC/ASIC proteins can form homomeric ion channels. The five proteins we studied, DEGT-1d, DEL-1d, UNC-8d, MEC-10d and MEC-4d, are expressed in three classes of mechanoreceptor neurons: touch receptor neurons (ALM, PLM, AVM, PVM), and polymodal nociceptors (ASH, PVD). Individual proteins were considered likely to form homomeric ion channels if total membrane current (measured at -85 mV) and its reversal potential differed from those measured in uninjected, control oocytes. We sought additional evidence by measuring ion selectivity and sensitivity to amiloride and its analogs as well as sensitivity to a panel of NSAIDs. To enhance constitutive currents and increase the

likelihood of detecting DEG/ENaC/ASIC-dependent currents, we used mutant or *d* isoforms of each of these proteins linked to neuronal degeneration.

**DEGT-1d, but not DEL-1d forms homomeric channels.**

Previous research showed that the DEG/ENaC/ASIC subunits MEC-4d and UNC-8d, but not MEC-10d can form homomeric channels when exogenously expressed in *Xenopus laevis* oocytes (Goodman et al., 2002; Wang et al., 2013). On average, oocytes expressing MEC-4d generated inward currents at -85 mV that were approximately 7-fold larger than those expressing UNC-8d and 17-fold larger than those expressing DEGT-1d. Oocytes expressing MEC-10d and DEL-1d, by contrast, generated currents that were indistinguishable from those recorded in uninjected oocytes (Fig. 1A-I, Table 1). Consistent with prior reports that oocytes expressing DEG/ENaC/ASIC channels become sodium loaded during the incubation period (Brown et al., 2007; Canessa et al., 1994; Goodman et al., 2002), membrane current reversed polarity near 0 mV in oocytes expressing MEC-4d and UNC-8d (Fig. 1C, 1D, 1I and Table 1). UNC-8d-expressing oocytes had more positive resting membrane potentials (Table 1) following incubation in a medium containing benzamil (100 μM) in addition to amiloride (300 μM), as expected from its low affinity for amiloride (see Fig. 4E). With these findings, we confirm prior work showing that MEC-4d and UNC-8d, but not MEC-10d forms homomeric channels in oocytes (Goodman et al., 2002; Wang et al., 2013) and show that DEL-1d is not likely to form ion channels on its own.

Oocytes expressing DEGT-1d generated small currents at -85 mV and these currents reversed polarity at significantly more positive potentials than those recorded from uninjected cells and those expressing MEC-10d and DEL-1d. The reversal potential of DEGT-1d currents was also significantly more negative than those recorded from cells expressing MEC-4d and UNC-8d (Fig. 1 E-I and Table 1). Together, these findings suggest that DEGT-1d is sufficient to generate an ion channel whose properties differ from channels formed by MEC-4d and UNC-8d. To verify that DEGT-1d is able to form homomeric channels, we sought recording conditions in which the current could be potentiated or blocked. As other members of this superfamily form acid-sensitive ion channels, we tested the effect of changing pH on currents carried by DEGT-1d, MEC4-d, UNC-8d. Switching from solutions from pH 8.4 to 6.4 decreased current carried by DEGT-1d and, to a lesser degree, MEC-4d (Fig. 1J). By contrast, acidification appeared to

potentiate UNC-8d currents (Fig. 1J). Collectively, these findings indicate that DEGT-1d forms a homomeric channel with properties that differ from most other DEG/ENaC/ASIC channels and suggest that alkalization could enhance DEGT-1-dependent currents *in vivo*.

<insert Figure 1 near here>

<Insert Table 1 near here>

**Unlike MEC-4d and UNC-8d, DEGT-1d channels are not sodium selective**

Most of the DEG/ENaC/ASIC channels studied experimentally are more permeable to $Na^+$ ions than $K^+$ ions. ENaCs are strongly sodium-selective with permeability ratio, $P_{Na}/P_K$, values exceeding 100 (Kellenberger et al., 1999; Palmer, 1987). ASICs exhibit much lower $P_{Na}/P_K$ ratios of 1-14 (Gründer and Pusch, 2015; Voilley, 2004). The reversal potential of homomeric DEGT-1d channels compared to MEC-4d and UNC-8d suggested to us that DEGT-1d channels differ in their ion permeability properties. We addressed this question by measuring the relative permeability of DEGT-1, UNC-8d, and MEC-4d to a series of monovalent cations (Fig. 2). The permeability of DEGT-1d is dramatically different from MEC-4d and UNC-8d with $P_{Na} \approx P_K \approx P_{Cs} > P_{Li} > P_{NMG}$ (Fig. 2A, Table 2). The permeability of UNC-8d is similar to MEC-4d: $P_{Li} > P_{Na} > P_K \approx P_{Cs} \approx P_{NMG}$ (Fig. 2B, Table 2). Our results differ from prior reports that UNC-8d channels are less permeable to $Li^+$ ions than they are to $Na^+$ ions (Wang et al., 2013). This discrepancy may stem from inferring permeability from current amplitude (Wang et al., 2013) *vs.* bi-ionic changes in reversal potential (this study). The permeability of codon-optimized MEC-4d to $Li^+$, $K^+$, $Cs^+$, and $NMG^+$ relative to $Na^+$, $P_x/P_{Na}$ was similar to prior studies of MEC-4d encoded by the native *C. elegans* codons (Brown et al., 2007; Goodman et al., 2002) with $P_{Li} > P_{Na} > P_K \approx P_{Cs} \approx P_{NMG}$ (Fig. 2C, Table 2). Thus, cRNAs derived from codon-optimized expression plasmids generate ion channels with properties that are indistinguishable from those derived from native sequences. To our knowledge, DEGT-1d is the first DEG/ENaC/ASIC subunit which is equally permeable to $K^+$ and $Na^+$, a finding which has implications for the *in vivo* function of this channel as well as for variations in biophysical properties within the DEG/ENaC/ASIC superfamily.

<insert Figure 2 near here>

<Insert Table 2 near here>

**Unlike MEC-4d and UNC-8d, DEGT-1d is insensitive to amiloride analogs**

The DEG/ENaC/ASIC ion channel family is also known as the amiloride-sensitive ion channel (ASC) family (Goodman and Schwarz, 2003; Hanukoglu and Hanukoglu, 2016; Kellenberger and Schild, 2002), suggesting that channels formed by these proteins are sensitive to the diuretic amiloride and its derivatives. Indeed, both MEC-4d and UNC-8d are known to be blocked by amiloride (Goodman et al., 2002; Wang et al., 2013). MEC-4d has a micromolar affinity for amiloride and UNC-8d is 45-fold less sensitive to amiloride (Brown et al., 2007; Goodman et al., 2002). To learn more about amiloride block as a shared, but potentially variable property of DEG/ENaC/ASIC channels, we tested DEGT-1d, UNC-8d, and MEC-4d for sensitivity to amiloride (Amil) and four analogs: benzamil (Bmil), 5-(N-Ethyl-N-isopropyl)amiloride (EIPA), phenamil (Phen), and benzamidine (Bzd) (Fig. 3, top row). These analogs were developed in an effort to generate specificity for ENaCs and $Na^+/H^+$ antiporters, both of which play critical roles in the mammalian kidney and are inhibited by amiloride (Frelin et al., 1987).

<insert Figure 3 near here>
<insert Figure 4 near here>

For testing purposes, we exposed oocytes expressing DEGT-1d, UNC-8d, and MEC-4d to a single concentration (30 µM) of each amiloride analog. Figure 4A-C show responses of each channel to EIPA. Unlike MEC-4d, UNC-8d and most other DEG/ENaC/ASIC channels, DEGT-1d was insensitive to all amiloride analogs we tested at our reference concentration of 30 µM (Fig. 4D). To differentiate between a reduced affinity and a lack of sensitivity, we tested concentrations up to 300 µM for amiloride (the highest possible soluble concentration). At this concentration, amiloride showed a slight effect in DEGT-1 expressing oocytes with a mean change in current to uninjected oocytes of 60 nA. At a dose of 100 µM, neither amiloride nor benzamil produced a detectable change in current in either DEGT-1d-expressing or uninjected oocytes.

UNC-8d is inhibited not only by amiloride and benzamil (Wang et al., 2013, Miller-Flemming et al., 2016), but also by EIPA, phenamil and benzamidine (Fig. 4E). None of these compounds had any detectable effect on currents measured in control (uninjected) oocytes. Thus, these measured drug-sensitive currents are likely to be carried entirely by UNC-8d or MEC-4d. Amiloride analogs block UNC-8d currents with different degrees of potency. In ascending order of potency, UNC-8d was blocked by amiloride, phenamil, benzamidine, EIPA and benzamil. The reported $IC_{50}$ values for UNC-8d channels for amiloride at -100 mV are 7.8 μM in divalent and 106 μM in divalent free solution (Wang et al., 2013). The reported $IC_{50}$ values for UNC-8d channels for benzamil at -100 mV are 47 μM in divalent and 119 μM in divalent free solution (Miller-Flemming et al., 2016). In this study, we determined an $IC_{50}$ for benzamil in control saline (divalent solution) of 14.8 ± 1.6 μM (n =4) at -60 mV (15.1 μM at -100 mV) (Supplementary Fig. 1A-C). In contrast to amiloride inhibition, the apparent affinity to benzamil was indistinguishable at voltages between -100 and -20 mV, indicating that the block through benzamil is not voltage-dependent.

Similar to UNC-8d, MEC-4d is inhibited not only by amiloride, benzamil and benzamidine (Brown et al., 2007), but also by EIPA and phenamil. However, the order of potency differs from UNC-8d. In ascending order of apparent potency: MEC-4d was blocked by benzamidine < amiloride ≈ EIPA ≈ phenamil < benzamil. The similar potency of amiloride and EIPA was unexpected and we analyzed this drug further by collecting full dose-response curves for EIPA inhibition of MEC-4d (Supplementary Fig. 1D-E). The half-blocking dose or $IC_{50}$ for EIPA was 3.06 ± 0.6 μM (n = 11) at -60 mV (Supplementary Fig. 1E), which is indistinguishable from the $IC_{50}$ for amiloride (2.35 ± 0.39 μM (n = 7) at -60 mV (Brown et al., 2007). It has been shown that the block through amiloride in ENaC, MEC-4d and UNC-8d depends on the transmembrane potential difference in such a way that hyperpolarization of the membrane increases channel block (Kellenberger & Schild 2002, Brown 2007, Wang 2013). The apparent affinity to EIPA was indistinguishable at voltages between -100 and -20 mV (Supplementary Fig. 1F). Thus, at the voltages tested, the block of MEC-4d current with EIPA is not voltage-dependent, in contrast to the block with amiloride. Collectively, these results show that MEC-4d is blocked by many amiloride analogs, in order of potency: benzamidine (196 μM) < EIPA (3.06 μM, this study) ≈ amiloride (2.35 μM) ≈ phenamil (TBD) < benzamil (0.83 μM) (Brown, 2007).

If all of these drugs were to function as open channel blockers like amiloride, then the dramatic difference in the potency of amiloride-related drugs among DEGT-1d, UNC-8d and MEC-4d channels implies that these channels differ in the molecular pathways by which drugs access their presumptive binding site or the nature of the binding site in the ion conduction pathway. The former idea seems more likely since the conserved second transmembrane domain of DEG/ENaC/ASIC proteins has long been thought to line the ion conduction pore (Kellenberger et al., 1999; Snyder et al., 1999).

<Insert Figure 5 near here>

**NSAIDs have modest effects on DEGT-1d and UNC-8d, but potentiate MEC-4d.**

Because nonsteroidal anti-inflammatory drugs (NSAIDs) have been reported to block ASIC channels with $IC_{50}$ values in the high micromolar range (90-350 μM) (Lingueglia and Lazdunski, 2013; Voilley, 2004), we also examined sensitivity to NSAID drugs (ibuprofen (Ibu), flurbiprofen (Fibu), diclofenac (Diclo), aspirin (Asp) and salicylic acid (SA) (Fig. 3, bottom row) as an additional window into shared, but variable properties of DEG/ENaC/ASIC channels.

The five NSAIDS tested had either no detectable effect on DEGT-1d and UNC-8d currents or produced a small inhibitory effect at 30 μM (Fig. 5D, 5E). Flurbiprofen (Fig. 5A, 5D) and salicylic acid (Fig. 5D) blocked DEGT-1d current, while flurbiprofen (Fig. 5B, 5E) and diclofenac (Fig. 5E) blocked UNC-8d current. Surprisingly, all five NSAIDs potentiated the MEC-4d currents (Fig. 5C, 5F). These findings demonstrate that NSAIDs can function as antagonists or agonists of DEG/ENaC/ASIC channels, depending on the specific channel target.

<insert Figure 6 near here>

Next, we collected dose-response curves for two NSAIDs (ibuprofen and aspirin) applied to cells expressing MEC-4d channels. To improve the sensitivity of these measurements, we reduced the baseline currents by injecting 1.6-fold less cRNA encoding MEC-4d for these experiments. The mean $EC_{50}$ (± SEM) for ibuprofen and aspirin at -100 mV are 34.6 ± 0.9 μM (n = 12) and 79.9 ± 3.7 μM (n = 9), respectively (Fig. 6A). Neither drug showed evidence of voltage-dependence (Fig. 6B), suggesting that the binding site for these drugs lies outside the

pore region. Ibuprofen is an enantiomer containing two chiral molecules and the S-isoform is the preferred ligand for its primary targets, the cyclo-oxygenase enzymes, COX-1 and COX-2 (Orlando et al., 2015; Selinsky et al., 2001). In contrast, MEC-4d potentiation is equally sensitive to both ibuprofen enantiomers (Fig. 6C) and is less sensitive to ibuprofen than COX-1 and COX-2 (Blobaum and Marnett, 2007). Collectively, these findings suggest that the bindings sites for NSAIDs differ in DEG/ENaC/ASIC channels and cyclo-oxygenases.

MEC-4d is not the only DEG/ENaC/ASIC channel affected by NSAIDs. rASIC1a is inhibited by ibuprofen and this allosteric effect depends on three positively charged and two hydrophobic residues near TM1 and TM2 (Fig. 6D-E) (Lynagh et al., 2017b). To learn more about the putative binding site for ibuprofen, which is proposed to include these five residues, we aligned and compared the sequences of seven *C. elegans* DEG/ENaC/ASIC channels with rASIC1a (Fig. 6E). We found that MEC-4 differs from rASIC1a at the three of these residues (Fig. 6E, arrowheads). Here, we focused on K422 in rASIC1a and E704, the glutamate at the homologous position in MEC-4 (Fig. 6E, black arrowhead). Comparing the effect of ibuprofen on MEC-4d and MEC-4d[E704K], we found that ibuprofen potentiated both isoforms to a similar extent (Fig. 6F-H). The $EC_{50}$ for ibuprofen was modestly increased in MEC-4d[E704K], but unaffected in MEC-4d[E704A] (Fig. 6I). The mean $EC_{50}$ (± SEM) to ibuprofen for MEC-4d[E704K] and MEC-4d[E704A] at -100 mV are 135 ± 40 μM (n = 13) and 19.5 ± 8.84 μM (n = 14), respectively (Fig. 6I). A similar shift was observed for potentiation for MEC-4d[E704K] by aspirin with a mean $EC_{50}$ (± SEM) of 179 ± 56 μM (n = 9) (Fig. 6J). This differs from allosteric inhibition of rASIC1a, which is significantly impaired by introducing alanine into this position (Lynagh et al., 2017b). In an effort to learn more about the channel domains responsible for these differences between rASIC1a and MEC-4d, we designed constructs encoding chimeras of these two channels. These chimeras did not generate any detectable current even when co-expressed with MEC-2. Nevertheless, these findings imply that the NSAIDs share a similar binding site in MEC-4d to the one proposed for rASIC1a and ibuprofen binding cause either inhibition or activation.

## Discussion

*DEG/ENaC/ASIC channels differ in their ion selectivity*

DEG/ENaC/ASIC channels are generally considered to be sodium-selective ion channels, but are also permeable to alkali metal ions in descending order of relative permeability, $Li^+>Na^+>K^+>Cs^+$. Members of this family of ion channels differ in their selectivity for $Na^+$ over $K^+$ ions. The ENaC channels are 100-fold more permeable to $Na^+$ than to $K^+$ and ASIC channels have permeability ratios in the range of 5-14 [reviewed in (Gründer and Pusch, 2015)]. The relative permeability of MEC-4d and UNC-8d (Table 2) is similar to that found for ASIC channels, but DEGT-1 is slightly more permeable to $K^+$ than it is to $Na^+$ or $Li^+$ ions (Fig. 2, Table 2). Together with other studies (Li et al., 2011; Lynagh et al., 2017a), this unexpected finding suggests DEG/ENaC/ASIC channels select among cations using a mechanism that is more complex than the size of the dehydrated or hydrated ion.

There are elements of the DEGT-1 sequence and structure might account for this difference in selectivity. The conserved TM2 domain forms the ion conduction pore of all DEG/ENaC/ASIC channels and ionic selectivity was initially proposed to depend on a conserved GAS motif (Kellenberger et al., 1999; Snyder et al., 1999), that forms the narrowest part of the pore in crystal structures (Baconguis et al., 2014). Recent studies of the energetics of permeation suggest that this motif contributes a barrier to $K^+$ permeation, but is not the locus of $Na^+$ selectivity (Lynagh et al., 2017a). In DEGT-1, this motif is modified to GAT (Fig. 6E), raising the possibility this variation reduces the barrier to $K^+$ permeation. In crystal structures of ASIC1a, these three amino acids are in an extended conformation and divide TM2 into an upper, extracellular sub-helix (TM2a) and a lower, intracellular sub-helix (TM2b) that associates with the TM2a of the neighboring subunit (Baconguis et al., 2014). Residues in both TM2a and TM2b are known to contribute to ion selectivity in several DEG/ENaC/ASIC channels (Árnadóttir et al., 2011; Li et al., 2011; Lynagh et al., 2017a; O'Hagan et al., 2005), indicating that the GAS motif is not the sole determinant of selectivity. The primary sequence of TM2b in DEGT-1 is more divergent than that of TM2a (Fig. 6E), suggesting that the variation in TM2b might account for increased permeability to $K^+$. The sequence divergence in TM2b is not unique to DEGT-1, however. A large-scale analysis of ASIC channels reveals many co-evolving residue pairs in TM2a and fewer co-evolving residue pairs in TM2b, indicative of increased evolutionary divergence (Kasimova et al., 2019).

The intracellular N-terminal domain also contributes to ion selectivity (Árnadóttir et al., 2011; Coscoy et al., 1999). Most of the high-resolution structures of ASIC1a have used truncated

proteins or failed to resolve the N-terminal region. A recent study has now resolved this domain of cASIC1a with ~2.8 and 3.5 Å resolution and reports that it folds into the pore region such that a highly conserved HG motif tucks into the bottom of the GAS motif (Yoder and Gouaux, 2020) (Fig. 6E, dark grey background). Interestingly, the histidine in this motif is conserved in ASICs and ENaCs, but also in most *C. elegans* DEG channels, except for DEGT-1 and a few others. DEGT-1 carries a leucine residue at the respective position (Fig. 6E). Future work systematically investigating the contribution of the DEGT-1 N-terminal, TM1 and TM2b to ion selectivity could deepen understanding of in DEG/ENaC/ASIC channels more broadly.

*Sensitivity to amiloride and its analogs*

Developed in 1967 to treat hypertension, amiloride is listed an essential medicine by the world health organization (World Health Organization, 2019). Many amiloride derivatives have been developed and we leveraged this collection of potential inhibitors to evaluate the sensitivity of DEGT-1d, UNC-8d and MEC-4d to a panel of five amiloride analogs (Fig. 4). Whereas both MEC-4d and UNC-8d were inhibited by at least one amiloride analog, DEGT-1d was not obviously affected by any of the five amiloride analogs we tested. UNC-8d currents differed from MEC-4d in their sensitivity to amiloride analogs. In particular, UNC-8d currents are more sensitive to inhibition by benzamil and EIPA than to either amiloride or phenamil. Four of the five compounds inhibited currents carried by MEC-4d at a constant dose of 30 µM. [Benzamidine had little or no effect on MEC-4d at this concentration, but does block MEC-4d currents at higher doses (Brown et al., 2007).] Benzamil was the most potent inhibitor of MEC-4d currents, followed by amiloride, EIPA, and phenamil (Fig. 4F, (Brown et al., 2007)). Single-channel recordings demonstrate that amiloride functions as an open channel blocker of MEC-4 channels (Brown et al., 2007), indicating that amiloride binds within the ion conduction pore. This idea is reinforced by three-dimensional co-crystal structures of cASIC1a and amiloride revealing an amiloride molecule lodged near the external vestibule of the central pore (Baconguis et al., 2014). Together, our findings suggest that DEGT-1d, UNC-8d, and MEC-4d proteins form homomeric channels that differ in the structure of the amiloride binding site or in the accessibility of compounds to this site.

*Sensitivity to NSAIDs and their analogs*

The primary function of non-steroidal anti-inflammatory drugs or NSAIDs is to inhibit prostaglandin synthesis by inhibiting cyclo-oxygenase-1 (COX-1) and COX-2 enzymes (Day and Graham, 2013; Weissmann, 1991). These compounds also inhibit DEG/ENaC/ASIC channels (Lingueglia and Lazdunski, 2013; Voilley, 2004; Voilley et al., 2001) and this effect may contribute to their efficacy as analgesic agents. In particular, ibuprofen decreases proton-gated currents carried by rASIC1a channels and sensitivity to ibuprofen depends on residues in the extracellular domain positioned within a pocket of positively charged and aromatic residues near the transmembrane domains (Lynagh et al., 2017b). Building on this finding, we tested our channels for sensitivity to five NSAIDS at a constant 30μM dose (Fig. 5F, Fig. 6). Only one out of five modestly inhibited DEGT-1d (Fig. 5D) and UNC-8d (Fig. 5E), whereas all of these compounds strongly activated MEC-4d currents (Fig. 5F).

The NSAID ibuprofen potentiates MEC-4d currents in a dose-dependent manner (Fig. 6A), but functions as a negative allosteric modulator of proton-gated ASIC1a currents (Lynagh et al., 2017b). Based on our finding that mutating E704 decreases the apparent affinity for ibuprofen (Fig. 6I), we propose that MEC-4d shares an analogous ibuprofen binding site with ASIC1a. This raises the question of how ibuprofen binding might enhance MEC-4d current and suppress ASIC1a current. In ASIC1a, ibuprofen and protons elicit opposing conformational changes at the top of the pore-lining second transmembrane domain (Lynagh et al., 2017b), supporting the idea that ibuprofen is a negative allosteric modulator of proton-dependent ASIC1a gating. If a similar conformational change were associated with NSAID binding to MEC-4d, then it would be uncoupled to proton binding (MEC-4d is not activated by protons) and we would infer that the motion is associated with an increase in channel gating. Future work will be needed to resolve the exact nature of the allosteric interactions between ibuprofen binding and channel gating, however. The differential response of MEC-4d and ASIC1a presents an avenue for further study.

<Insert Fig 7 here>

*Concluding remarks*

The DEG/ENaC/ASIC channels are unique: unlike any other classes of ion channels, they are only present in metazoan genomes (Katta et al., 2015; Liebeskind et al., 2015). Phylogenetic studies indicate that this gene superfamily has undergone expansions within certain animal

lineages, including nematodes and insects (Liebeskind et al., 2015). Based on the initial structure of ASIC1a, the extracellular domain of these channels is divided into subdomains resembling the parts of a hand—including thumb, palm, finger and knuckle (Jasti et al., 2007).The finger domain is positioned furthest away from the plasma membrane and shows the highest variability (Eastwood and Goodman, 2012; Kashlan and Kleyman, 2011) Although the significance of these variations is not fully understood, the GRIP (Gating Relief of Inhibition by Proteolysis) sub-domain resides within the finger domain, enables the activation of ENaCs by proteolysis [reviewed by (Rossier and Stutts, 2009), and is unique to ENaCs (Noreng et al., 2018).

By analyzing a subset of *C. elegans* DEG/ENaC/ASIC proteins, we extend understanding of the functional diversification of this ion channel superfamily. In particular, we show that DEGT-1 is equally permeable to $K^+$ than $Na^+$ and has no significant response to amiloride or the four derivatives we tested. To our knowledge, this is the first member of this family to have these properties. From the subset of DEG/ENaC/ASIC studied, interestingly DEGT-1 phylogenetically distant from the others tested (Fig. 7). We also identified NSAIDs as potential inhibitors of DEGT-1d currents and positive modulators of MEC-4d currents. Collectively, we demonstrate that each of the proteins able to form homomeric channels in Xenopus oocytes exhibits a unique pharmacological footprint within two drug families.

**Acknowledgements**

We thank Z. Liao for excellent technical support, including Xenopus oocyte isolation and molecular biology; L. Bianchi for the gift of the UNC-8-encoding plasmid. This work was funded by fellowship to SF (DFG), the Amgen Scholars Program to ID (SSRP), and grants from NIH to MBG (R01NS07715, R35NS105092).Work by LT was supported by the Howard Hughes Medical Institute.

**References**


Adams, C.M., Snyder, P.M., Welsh, M.J., 1999. Paradoxical stimulation of a DEG/ENaC channel by amiloride. J. Biol. Chem. 274, 15500–15504. doi:10.1074/jbc.274.22.15500

Árnadóttir, J., O'Hagan, R., Chen, Y., Goodman, M.B., Chalfie, M., 2011. The DEG/ENaC protein MEC-10 regulates the transduction channel complex in Caenorhabditis elegans touch receptor neurons. J. Neurosci. 35, 12695–12704. doi:10.1523/JNEUROSCI.4580-10.2011

Baconguis, I., Bohlen, C.J., Goehring, A., Julius, D., Gouaux, E., 2014. X-ray structure of acid-sensing ion channel 1-snake toxin complex reveals open state of a $Na^+$-selective channel. Cell 156, 717–729. doi:10.1016/j.cell.2014.01.011

Blobaum, A.L., Marnett, L.J., 2007. Structural and functional basis of cyclooxygenase inhibition. J. Med. Chem. 50, 1425–1441. doi:10.1021/jm0613166

Boscardin, E., Alijevic, O., Hummler, E., Frateschi, S., Kellenberger, S., 2016. The function and regulation of acid-sensing ion channels (ASICs) and the epithelial $Na^+$ channel (ENaC): IUPHAR Review 19. Br. J. Pharmacol. 2671–2701. doi:10.1111/bph.13533

Brown, A.L., Fernandez-Illescas, S.M., Liao, Z., Goodman, M.B., 2007. Gain-of-function mutations in the MEC-4 DEG/ENaC sensory mechanotransduction channel alter gating and drug blockade. J. Gen. Physiol. 129, 161-q73. doi:10.1085/jgp.200609672

Canessa, C.M., Horisberger, J.D., Schild, L., Rossier, B.C., 1995. Expression cloning of the epithelial sodium channel, in: Kidney International. Department of Cellular and Molecular Physiology, Yale School of Medicine, New Haven, Connecticut, USA., pp. 950–955. doi:10.1038/ki.1995.376

Canessa, C.M., Schild, L., Buell, G., Thorens, B., Gautschi, I., Horisberger, J.-D., Rossier, B.C., 1994. Amilorid-sensitive epithelial Na+ channel is made of three homologous subunits. Nature 370, 621–628. doi:doi:10.1038/367463a0

Chalfie, M., Chelur, Dattananda, S., Ernstrom, G.G., O'Hagan, R., Yao, C.A., Goodman, M.B., 2003. METHODS AND COMPOSITIONS FOR PROPAGATING VECTORS CONTAINING TOXIC cDNAs AND ION CHANNEL ASSAY SYSTEMS. WO2003060093A2.

Chalfie, M., Wolinsky, E., 1990. The identification and suppression of inherited neurodegeneration in Caenorhabditis elegans. Nature 345, 410–416. doi:10.1038/345410a0

Chatzigeorgiou, M, Grundy, L., Kindt, K.S., Lee, W.-H., Driscoll, M., Schafer, W.R., 2010. Spatial Asymmetry in the Mechanosensory Phenotypes of the C. elegans DEG/ENaC Gene mec-10. J. Neurophysiol. 104, 3334–3344.

Chatzigeorgiou, Marios, Yoo, S., Watson, J.D., Lee, W.H., Spencer, W.C., Kindt, K.S., Hwang, S.W., Miller, D.M., Treinin, M., Driscoll, M., Schafer, W.R., 2010. Specific roles for DEG/ENaC and TRP channels in touch and thermosensation in *C. elegans* nociceptors. Nat. Neurosci. 13, 861–868. doi:10.1038/nn.2581

Coscoy, S., De Weille, J.R., Lingueglia, E., Lazdunski, M., 1999. The pre-transmembrane 1 domain of acid-sensing ion channels participates in the ion pore. J. Biol. Chem. 274, 10129–10132. doi:10.1074/jbc.274.15.10129

Dawson, R.J.P., Benz, J., Stohler, P., Tetaz, T., Joseph, C., Huber, S., Schmid, G., Hügin, D., Pflimlin, P., Trube, G., Rudolph, M.G., Hennig, M., Ruf, A., 2012. Structure of the Acid-sensing ion channel 1 in complex with the gating modifier Psalmotoxin 1. Nat. Commun. 3. doi:10.1038/ncomms1917

Day, R.O., Graham, G.G., 2013. Therapeutics: Non-steroidal anti-inflammatory drugs (NSAIDs). BMJ 347, 1–7. doi:10.1136/bmj.f3195

Dereeper, A., Audic, S., Claverie, J.M., Blanc, G., 2010. BLAST-EXPLORER helps you building datasets for phylogenetic analysis. BMC Evol. Biol. 10, 8–13. doi:10.1186/1471-2148-10-8

Dereeper, A., Guignon, V., Blanc, G., Audic, S., Buffet, S., Chevenet, F., Dufayard, J.F., Guindon, S., Lefort, V., Lescot, M., Claverie, J.M., Gascuel, O., 2008. Phylogeny.fr: robust phylogenetic analysis for the non-specialist. Nucleic Acids Res. 36, 465–469. doi:10.1093/nar/gkn180

Driscoll, M., Chalfie, M., 1991. The mec-4 gene is a member of a family of Caenorhabditis elegans genes that can mutate to induce neuronal degeneration. Nature 354, 56–58.

Eastwood, A.L., Goodman, M.B., 2012. Insight into DEG/ENaC channel gating from genetics and structure. Physiology (Bethesda). 27, 282–90. doi:10.1152/physiol.00006.2012

Elkhatib, W., Smith, C.L., Senatore, A., 2019. A Na+ leak channel cloned from trichoplax adhaerens extends extracellular pH and Ca2+ sensing for the DEG/ENaC family close to the base of Metazoa. J. Biol. Chem. 294, 16320–16336. doi:10.1074/jbc.RA119.010542

Frelin, C., Vigne, P., Barbry, P., Lazdunski, M., 1987. Molecular properties of amiloride action

and of its Na + transporting targets. Kidney Int. 32, 785–793. doi:10.1038/ki.1987.277

García-Añoveros, J., Derfler, B., Neville-Golden, J., Hyman, B.T., Corey, D.P., 1997. BNaC1 and BNaC2 constitute a new family of human neuronal sodium channels related to degenerins and epithelial sodium channels. Proc. Natl. Acad. Sci. U. S. A. 94, 1459–1464. doi:10.1073/pnas.94.4.1459

Garty, H., Benos, D.J., 1988. Characteristics and regulatory mechanisms of the amiloride-blockable Na+ channel. Physiol. Rev. 68, 309–362. doi:10.1016/S0140-6736(01)19886-7

Gonzales, E.B., Kawate, T., Gouaux, E., 2009. Pore architecture and ion sites in acid-sensing ion channels and P2X receptors. Nature 460, 599–604. doi:10.1038/nature08218

Goodman, M.B., Ernstrom, G.G., Chelur, D.S., Hagan, R.O., Yao, A.C., Chalfie, M., 2002. MEC-2 regulates *C . elegans* DEG / ENaC channels needed for mechanosensation. Lett. to Nat. 415, 1039–1042.

Goodman, M.B., Schwarz, E.M., 2003. Transducing touch in Caenorhabditis elegans. Annu. Rev. Physiol. 65, 429–452. doi:10.1146/annurev.physiol.65.092101.142659

Gründer, S., Pusch, M., 2015. Biophysical properties of acid-sensing ion channels (ASICs). Neuropharmacology. doi:10.1016/j.neuropharm.2014.12.016

Hanukoglu, I., Hanukoglu, A., 2016. Epithelial sodium channel (ENaC) family: Phylogeny, structure-function, tissue distribution, and associated inherited diseases. Gene 579, 95–132. doi:10.1016/j.gene.2015.12.061

Hille, B., 2001. Ion Channels of Excitable Membranes, 3rd ed. Sinauer Associates, Sunderland, MA.

Ho, J., Tumkaya, T., Aryal, S., Choi, H., Claridge-Chang, A., 2019. Moving beyond P values: data analysis with estimation graphics. Nat. Methods 16, 565–566. doi:10.1038/s41592-019-0470-3

Hobert, O., 2013. The neuronal genome of Caenorhabditis elegans. WormBook. doi:10.1895/wormbook.1.161.1

Huang, M., Chalfie, M., 1994. Gene interactions affecting mechanosensory transduction in Caenorhabditis elegans. Nature 367, 467–470.

Jasti, J., Furukawa, H., Gonzales, E.B., Gouaux, E., 2007. Structure of acid-sensing ion channel 1 at 1.9 Å resolution and low pH. Nature 449, 316–323. doi:10.1038/nature06163

Kashlan, O.B., Kleyman, T.R., 2011. ENaC structure and function in the wake of a resolved

structure of a family member. Am. J. Physiol. - Ren. Physiol. 301, 684–696. doi:10.1152/ajprenal.00259.2011

Kasimova, M.A., Lynagh, T., Sheikh, Z.P., Granata, D., Borg, C.B., Carnevale, V., Pless, S.A., 2019. Evolutionarily Conserved Interactions within the Pore Domain of Acid-Sensing Ion Channels. Biophys. J. doi:10.1016/j.bpj.2019.09.001

Katta, S., Krieg, M., Goodman, M.B., 2015. Feeling Force: Physical and Physiological Principles Enabling Sensory Mechanotransduction, in: Annual Review of Cell and Developmental Biology. doi:10.1146/annurev-cellbio-100913-013426

Kellenberger, S., Gautschi, I., Schild, L., 1999. A single point mutation in the pore region of the epithelial Na+ channel changes ion selectivity by modifying molecular sieving. Proc. Natl. Acad. Sci. U. S. A. 96, 4170–4175. doi:10.1073/pnas.96.7.4170

Kellenberger, S., Schild, L., 2015. International Union of Basic and Clinical Pharmacology. XCI. Structure, Function, and Pharmacology of Acid-Sensing Ion Channels and the Epithelial Na+ Channel. Pharmacol. Rev. 67, 1–35. doi:10.1124/pr.114.009225

Kellenberger, S., Schild, L., 2002. Epithelial Sodium Channel/Degenerin Family of Ion Channels: A Variety of Functions for a Shared Structure. Physiol. Rev. 82, 735–767.

Li, T., Yang, Y., Canessa, C.M., 2011. Outlines of the pore in open and closed conformations describe the gating mechanism of ASIC1. Nat. Commun. 2, 399–405. doi:10.1038/ncomms1409

Liebeskind, B.J., Hillis, D.M., Zakon, H.H., 2015. Convergence of ion channel genome content in early animal evolution. Proc. Natl. Acad. Sci. U. S. A. 112, E846–E851.

Liman, E.R., Tytgat, J., Hess, P., 1992. Subunit stoichiometry of a mammalian K+ channel determined by construction of multimeric cDNAs. Neuron. doi:10.1016/0896-6273(92)90239-A

Lingueglia, E., Lazdunski, M., 2013. Pharmacology of ASIC channels. Wiley Interdiscip. Rev. Membr. Transp. Signal. 2, 155–171. doi:10.1002/wmts.88

Liu, X.S., Liu, X.J., 2006. Xenopus protocols cell biology and signal transduction, Methods in molecular biology (Clifton, N.J.). doi:10.1007/978-1-59745-000-3_32

Lynagh, T., Flood, E., Boiteux, C., Wulf, M., Komnatnyy, V. V, Colding, J.M., Allen, T.W., Pless, S.A., 2017a. A selectivity filter at the intracellular end of the acid-sensing ion channel pore. Elife 6, 1–21. doi:10.7554/eLife.24630

Lynagh, T., Romero-Rojo, J.L., Lund, C., Pless, S.A., 2017b. Molecular Basis for Allosteric Inhibition of Acid-Sensing Ion Channel 1a by Ibuprofen. J. Med. Chem. 60, 8192–8200. doi:10.1021/acs.jmedchem.7b01072

Matthewman, C., Johnson, C.K., Miller, D.M., Bianchi, L., 2018. Functional features of the "finger" domain of the DEG/ENaC channels MEC-4 and UNC-8. Am. J. Physiol. Physiol. 315, C155–C163. doi:10.1152/ajpcell.00297.2017

Matthewman, C., Miller-Fleming, T.W., Miller, D.M., Bianchi, L., 2016. Ca2+ permeability and Na+ conductance in cellular toxicity caused by hyperactive DEG/ENaC channels. Am. J. Physiol. - Cell Physiol. 311, C920–C930. doi:10.1152/ajpcell.00247.2016

Miller-Fleming, T.W., Petersen, S.C., Manning, L., Matthewman, C., Gornet, M., Beers, A., Hori, S., Mitani, S., Bianchi, L., Richmond, J., Miller, D.M., 2016. The DEG/ENaC cation channel protein UNC-8 drives activity-dependent synapse removal in remodeling GABAergic neurons. Elife 5, 1–28. doi:10.7554/eLife.14599

Noreng, S., Bharadwaj, A., Posert, R., Yoshioka, C., Baconguis, I., 2018. Structure of the human epithelial sodium channel by cryo-electron microscopy. Elife 7, 1–23. doi:10.7554/elife.39340

O'Hagan, R., Chalfie, M., Goodman, M.B., 2005. The MEC-4 DEG/ENaC channel of Caenorhabditis elegans touch receptor neurons transduces mechanical signals. Nat. Neurosci. 8, 43–50. doi:10.1038/nn1362

Orlando, B.J., Lucido, M.J., Malkowski, M.G., 2015. The structure of ibuprofen bound to cyclooxygenase-2. J. Struct. Biol. 189, 62–66. doi:10.1016/j.jsb.2014.11.005

Palmer, L., 1992. Epithelial Na Channels: Function And Diversity. Annu. Rev. Physiol. 54, 51–66. doi:10.1146/annurev.physiol.54.1.51

Palmer, L.G., 1987. Ion selectivity of epithelial Na channels. J. Membr. Biol. 96, 97–106. doi:10.1007/BF01869236

Rambaud, A., 2018. FigTree 1.4.4 Software [WWW Document]. URL http://tree.bio.ed.ac.uk/software/figtree/

Rossier, B.C., Stutts, M.J., 2009. Activation of the Epithelial Sodium Channel (ENaC) by Serine Proteases. Annu. Rev. Physiol. 71, 361–379. doi:10.1146/annurev.physiol.010908.163108

Schild, L., Schneeberger, E., Gautschi, I., Firsov, D., 1997. Identification of amino acid residues in the alpha, beta, and gamma subunits of the epithelial sodium channel (ENaC) involved in

amiloride block and ion permeation. J. Gen. Physiol. 109, 15–26. doi:10.1085/jgp.109.1.15

Selinsky, B.S., Gupta, K., Sharkey, C.T., Loll, P.J., 2001. Structural analysis of NSAID binding by prostaglandin H2 synthase: Time-dependent and time-independent inhibitors elicit identical enzyme conformations. Biochemistry 40, 5172–5180. doi:10.1021/bi010045s

Snyder, P.M., Olson, D.R., Bucher, D.B., 1999. A pore segment in DEG/ENaC Na+ channels. J. Biol. Chem. 274, 28484–28490. doi:10.1074/jbc.274.40.28484

Sun, D., Yu, Y., Xue, X., Pan, M., Wen, M., Li, S., Qu, Q., Li, Xiaorun, Zhang, L., Li, Xueming, Liu, L., Yang, M., Tian, C., 2018. Cryo-EM structure of the ASIC1a-mambalgin-1 complex reveals that the peptide toxin mambalgin-1 inhibits acid-sensing ion channels through an unusual allosteric effect. Cell Discov. 4. doi:10.1038/s41421-018-0026-1

Tavernarakis, N., Shreffler, W., Wang, S., Driscoll, M., 1997. unc-8, a DEG/ENaC family member, encodes a subunit of a candidate mechanically gated channel that modulates C. elegans locomotion. Neuron 18, 107–119. doi:10.1016/S0896-6273(01)80050-7

Voilley, N., 2004. Acid-sensing ion channels (ASICs): New targets for the analgesic effects of non-steroid anti-inflammatory drugs (NSAIDs). Curr. Drug Targets Inflamm. Allergy. doi:10.2174/1568010043483980

Voilley, N., De Weille, J., Mamet, J., Lazdunski, M., 2001. Nonsteroid anti-inflammatory drugs inhibit both the activity and the inflammation-induced expression of acid-sensing ion channels in nociceptors. J. Neurosci. 21, 8026–8033.

Vullo, S., Kellenberger, S., 2019. A molecular view of the function and pharmacology of acid-sensing ion channels. Pharmacol. Res. 0–1. doi:10.1016/j.phrs.2019.02.005

Waldmann, R., Champigny, G., Bassilana, F., Heurteaux, C., Lazdunski, M., 1997. A proton-gated cation channel involved in acid-sensing. Nature 386, 173–177. doi:10.1038/386173a0

Wang, Y., Matthewman, C., Han, L., Miller, T., Miller, D.M., Bianchi, L., 2013. Neurotoxic unc-8 mutants encode constitutively active DEG/ENaC channels that are blocked by divalent cations. J. Gen. Physiol. 142, 157–69. doi:10.1085/jgp.201310974

Weissmann, G., 1991. The actions of NSAIDs. Hosp. Pract. 26, 60-68+71. doi:10.1080/21548331.1991.11705279

World Health Organization, 2019. Additions and deletions of medicines on the WHO model lists of essential medicines: 1977-2017. World Health Organization. CC BY-NC-SA 3.0 IGO.

Yoder, N., Gouaux, E., 2020. Conserved His-Gly motif of acid-sensing ion channels resides in a

reentrant ‘loop’ implicated in gating and ion selectivity. bioRxiv. doi:https://doi.org/10.1101/2020.03.02.974154

Yoder, N., Yoshioka, C., Gouaux, E., 2018. Gating mechanisms of acid-sensing ion channels. Nature 555, 397–401. doi:10.1038/nature25782

**Table 1: Mean values and estimation statistics supporting the conclusion that DEG/ENaC/ASIC subunits DEGT-1d, UNC-8d and MEC-4d form homomeric channels in *Xenopus* oocytes, while MEC-10 and DEL-1 likely do not.**

| **Channel** | $V_{rest}$ **(mV)** mean ± SEM (n) | $V_{rev}$ **(mV)** Mean ± SEM (n) | $\Delta V_{rev}$ **to uninjected (mV)** | **95%CI (mV)** | ***p*** | $I_m$ **at -85 mV (µA)** Mean ± SEM (n) | $\Delta I_m$ **to uninjected (uA)** | **95%CI (µA)** | ***p*** |
|---|---|---|---|---|---|---|---|---|---|
| | | | | | | | | | |
| MEC-4d | 13.61 ± 0.2 (95) | -1.85 ± 0.114 (93) | 47.20 | [38.4, 54.7] | 2.38E-25 | -10.81 ± 0.085 (95) | -10.7 | [-12.4, -9.14] | 4.53E-39 |
| UNC-8d | 6.93 ± 0.16 (56) | -3.67 ± 0.163 (59) | 52.80 | [44.2, 60.0] | 2.85E-20 | -1.68 ± 0.017 (59) | -1.57 | [-1.83, -1.33] | 1.15E-27 |
| DEGT-1d | -19.31 ± 0.1 (109) | -23.31 ± 0.140 (111) | 25.80 | [17.2, 33.3] | 9.05E-13 | -0.61 ± 0.004 (113) | -0.50 | [-0.58, -0.42] | 3.08e-34. |
| DEL-1d | -38.94 ± 0.9 (18) | -60.68 ± 1.563 (19) | -11.60 | [-26.0, 4.43] | 0.166 | -0.16 ± 0.008 (20) | -0.04 | [-0.13, 0.02] | 0.239 |
| MEC-10d | -27.31 ± 0.92 (19) | -42.12 ± 1.089 (19) | 6.96 | [-5.24, 18.7] | 0.251 | -0.21 ± 0.009 (19) | -0.09 | [-0.19, -0.03] | 0.004 |
| uninjected | -36.22 ± 0.12 | -49.08 ± 0.396 (95) | - | - | - | -0.12 ± 0.001 (144) | - | - | - |

| | | | | | | | | | |
|---|---|---|---|---|---|---|---|---|---|
| | (143) | | | | | | | | |

Mean values for the resting membrane voltage (Vrest), reversal potential ($V_{rev}$) and current ($I_m$) under voltage clamp conditions at the beginning of each recording session. $V_{rev}$ was calculated from the ramp protocol in Fig 1A and $I_m$ was measured within the same protocol at a -85mV step. Given are mean values ± SEM and number of experiments in parenthesis (n). Estimation statistics for Fig. 1H and 1I are described as a change in voltage ($\Delta V_{rev}$) and change in current ($\Delta I_m$) compared to uninjected oocytes, the 95% confidence interval [in mV or µA], and a two-sided p-value of the Mann-Whitney test.

**Table 2: Relative Permeability for DEGT-1d, UNC-8d and MEC-4d.**

| **Channel** | $\boldsymbol{P_{Li}}$ (mean [95% CI] (n)) | $\boldsymbol{P_K}$ | $\boldsymbol{P_{Cs}}$ | $\boldsymbol{P_{NMG}}$ |
|---|---|---|---|---|
| | | | | |
| MEC-4d | 1.26 [1.09, 1.42] (6) | 0.18 [0.13, 0.24] (7) | 0.07 [0.05, 0.09] (7) | 0.08 [0.04, 0.12] (6) |
| UNC-8d | 1.31 [1.11, 1.51] (11) | 0.34 [0.19, 0.48] (12) | 0.38 [0.1, 0.65] (12) | 0.24 [0.12, 0.36] (11) |
| DEGT-1d | 0.75 [0.71, 0.79] (10) | 1.09 [1.0, 1.18] (14) | 1.14 [1.07, 1.21] (10) | 0.49 [0.41, 0.57] (5) |

Ionic permeability relative to that for $Na^+$ (Px/PNa) was measured for indicated channels in two-electrode voltage clamp. Values are Px/PNa and are expressed as mean and the minimum and maximum values for the 95% confidence interval. Confidence interval were calculated in Python with DescrStatsW. Number of experiments are given in parenthesis (n). Two-way ANOVA followed by multiple comparison with the Holm-Sidak method ($P< 0.05$) resulted in the following order for Px/Na permeability within one protein: DEGT-1d: $K^+ = Cs^+ > Li^+ >$ NMG; UNC-8d: $Li^+ > K^+ = Cs^+ =$ NMG; MEC-4d: $Li^+ > K^+ = Cs^+ =$ NMG. Multiple comparison with a

the Holm-Sidak method ($P < 0.05$) resulted in the following order for Px/Na permeability across different ion channels and within one group of monovalent ions: $Li^+$: MEC-4d = UNC-8d > DEGT-1d; $K^+$: DEGT-1d > MEC-4d = UNC-8d; $Cs^+$: DEGT-1d > UNC-8d > MEC-4d; NMG: DEGT-1d > MEC-4d, DEGT-1d = UNC-8d, UNC-8d = MEC-4d.

**Table 3**: **Effect of amiloride anologs and NSAIDs on DEGT-1d currents relative to uninjected oocytes: estimations statistics supporting Fig. 4 and Fig. 5.**

| DEGT-1d | $\Delta I_m$ to uninjected (µA) | 95% CI (µA) | *p* |
|---|---|---|---|
| *amiloride analogs* | | | |
| amiloride | 0.0033 (20) | -0.02, 0.025 | 0.36 |
| benzamil | 0.0073 (18) | -0.009, 0.035 | 0.61 |
| EIPA | 0.0073 (13) | -0.008, 0.028 | 0.43 |
| phenamil | -0.0043 (13) | -0.024, 0.016 | 0.32 |
| benzamidine | 0.0041(13) | -0.012, 0.026 | 0.77 |
| *NSAIDs* | | | |
| ibuprofen | 0.02 (18) | 0.0068, 0.036 | 0.001 |
| flurbiprofen | 0.15 (5) | 0.084, 0.22 | 0.003 |
| diclofenac | -0.037 (5) | -0.075, -0.015 | 0.003 |
| aspirin | 0.037 (5) | 0.0075, 0.064 | 0.08 |
| salicylic acid | 0.073 (4) | 0.042, 0.094 | 0.006 |

Estimation statistics for Fig 4D and 5D are described as a change in current ($\Delta I_m$) compared to uninjected oocytes, the 95% confidence interval [µA], and a two-sided p-value of the Mann-Whitney test. Number of experiments are given in parenthesis (n).

**Table 4**: **Effect of amiloride anologs and NSAIDs on UNC-8d currents relative to uninjected oocytes: estimations statistics supporting Fig. 4 and Fig. 5.**

| UNC-8d | $\Delta I_m$ to uninjected (uA) | 95% CI (µA) | *p* |
|---|---|---|---|
| *amiloride analogs* | | | |
| amiloride | 0.22 (5) | 0.026, 0.29 | 0.03 |
| benzamil | 0.87 (18) | 0.64, 1.13 | 2.08e-09 |
| EIPA | 0.61 (9) | 0.45, 0.83 | 4.92e-06 |
| phenamil | 0.18 (10) | 0.12, 0.26 | 2.86e-06 |
| benzamidine | 0.32 (9) | 0.17, 0.58 | 1.29e-05 |
| *NSAIDs* | | | |
| ibuprofen | 0.026 (15) | 0.000518, 0.0492 | 0.024 |
| flurbiprofen | 0.22 (10) | 0.123, 0.382 | 0.00033 |
| diclofenac | 0.24 (13) | 0.156, 0.352 | 5.25e-06 |
| aspirin | -0.071 (9) | -0.162, 0.00864 | 0.39 |
| salicylic acid | -0.062 (10) | -0.197, 0.00931 | 0.16 |

Estimation statistics for Fig 4E and 5E are described as a change in current ($\Delta I_m$) compared to uninjected oocytes, the 95% confidence interval [µA], and a two-sided p-value of the Mann-Whitney test. Number of experiments are given in parenthesis (n).

**Table 5**: **Effect of amiloride anologs and NSAIDs on MEC-4d currents relative to uninjected oocytes: estimations statistics supporting Fig. 4 and Fig. 5.**

| MEC-4 | $\Delta I_m$ to uninjected (uA) | 95% CI (µA) | *p* |
|---|---|---|---|
| *amiloride analogs* | | | |
| amiloride | 6.71 (50) | 5.1, 8.87 | 2.07e-15 |
| benzamil | 7.81 (32) | 5.43, 11.0 | 2.03e-12 |
| EIPA | 5.53 (27) | 3.77, 8.11 | 2.07e-11 |
| phenamil | 5.18 (26) | 3.1, 8.08 | 2.02e-09 |
| benzamidine | 0.61 (25) | -0.065, 1.68 | 0.0022 |
| *NSAIDs* | | | |
| ibuprofen | -4.39 (9) | -6.43, -2.69 | 0.0015 |
| flurbiprofen | -3.7 (7) | -4.66, -2.92 | 0.0008 |
| diclofenac | -2.78 (24) | -4.44, -1.66 | 9.91e-08 |
| aspirin | -4.75 (6) | -7.73, -3.45 | 0.0014 |
| salicylic acid | -5.39 (7) | -7.26, -3.89 | 0.0008 |

Estimation statistics for Fig 4F and 5F are described as a change in current ($\Delta I_m$) compared to uninjected oocytes, the 95% confidence interval [µA], and a two-sided p-value of the Mann-Whitney test. Number of experiments are given in parenthesis (n).

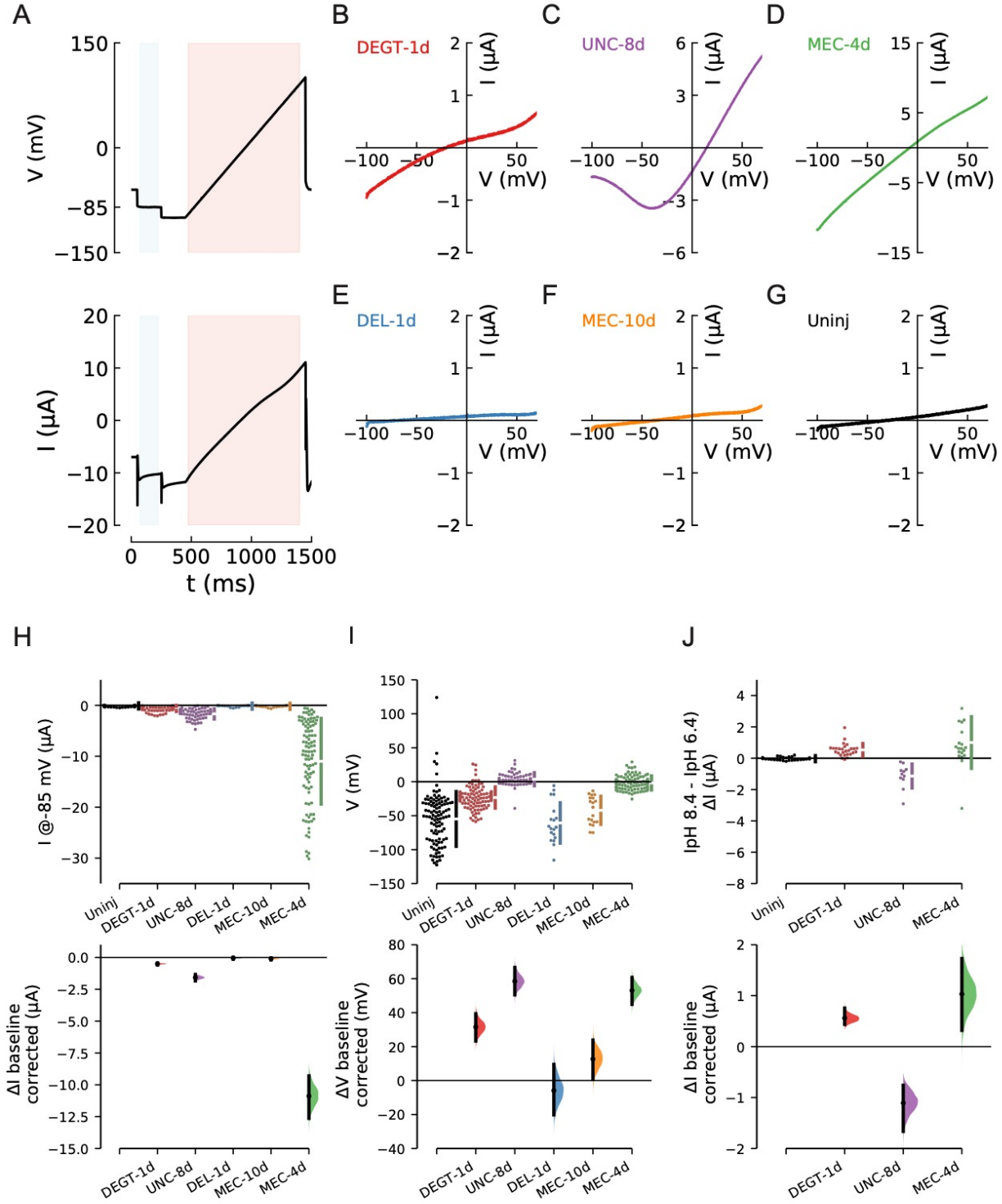
A
V (mV)
I (μA)
t (ms)
B
DEGT-1d
C
UNC-8d
D
MEC-4d
E
DEL-1d
F
MEC-10d
G
Uninj
I (μA)
V (mV)
H
I @-85 mV (μA)
I
V (mV)
J
IpH 8.4 - IpH 6.4
ΔI (μA)
ΔI baseline corrected (μA)
ΔV baseline corrected (mV)
Uninj
DEGT-1d
UNC-8d
DEL-1d
MEC-10d
MEC-4d

**FIG 1**

**Figure 1: The DEG/ENaC/ASIC subunits DEGT-1d, UNC-8d and MEC-4d form homomeric channels in Xenopus oocytes, while DEL-1d and MEC-10d likely do not. A:** Upper panel: Voltage protocol: from a holding potential of -60 mV, a step to -85 mV (grey background), followed by a step to -100 mV and a subsequent ramp protocol (red background) from -100 to 100 mV were applied while the oocytes were superfused with control saline. Lower panel: Current response to the above voltage protocol of a MEC-4d injected oocyte. **B-G:** IV curves of oocytes expressing DEGT-1d (**B**), UNC-8d (**C**), MEC-4d (**D**), DEL-1d (**E**), MEC-10d (**F**) and MEC-2 or uninjected oocytes (**G**). **H-I:** Estimation plot of current at -85 mV (grey background in A) (**H**) and voltage (**I**) of oocytes injected with DEG/ENaC/ASIC RNA compared to uninjected oocytes superfused with control saline. Statistics are described in Table 1. **J:** Estimation plot of the change in current at -85 mV (grey background in A) of oocytes injected with DEG/ENaC/ASIC RNA compared to uninjected oocytes exposed to change in pH in Gluconate-based solution from 8.4 to 6.4. Subsequent estimation statistics are described as a change in current compared to uninjected oocytes, the 95% confidence interval [in µA], and the two-sided p-value of the Mann-Whitney test: DEGT-1d: 0.56 µA [0.43, 0.76], p = 4.70E-09 (n = 27); UNC-8d: -1.11 µA, [-1.64, -0.76], 4.99E-07 (n = 11), MEC-4d: 1.03 µA [0.36, 1.78], 4.14E-06 (n = 20).

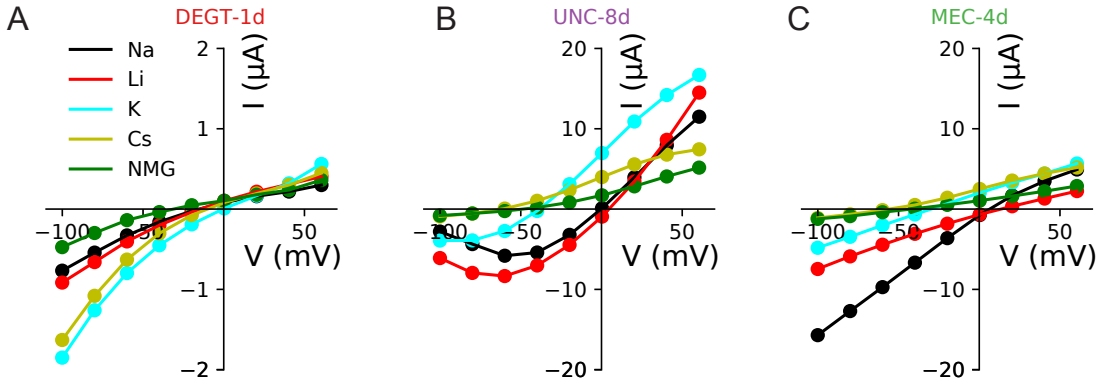


**FIG 2**

**Figure 2: DEGT-1d is equally permeable for $K^+$, $Cs^+$ and $Na^+$, while UNC-8d's relative permeability to monovalent ions is similar to MEC-4d. A-C:** Representative IV curves of oocytes expressing DEGT-1d (A), UNC-8d (B) or MEC-4d (C) together with MEC-2. Oocytes

were superfused with different Gluconate-based solutions, where the main ion was carried either by $Na^+$, $Li^+$, $K^+$, $Cs^+$ or NMG [100 mM]. Mean values +/- 95% confidence interval of population data in Table 2.

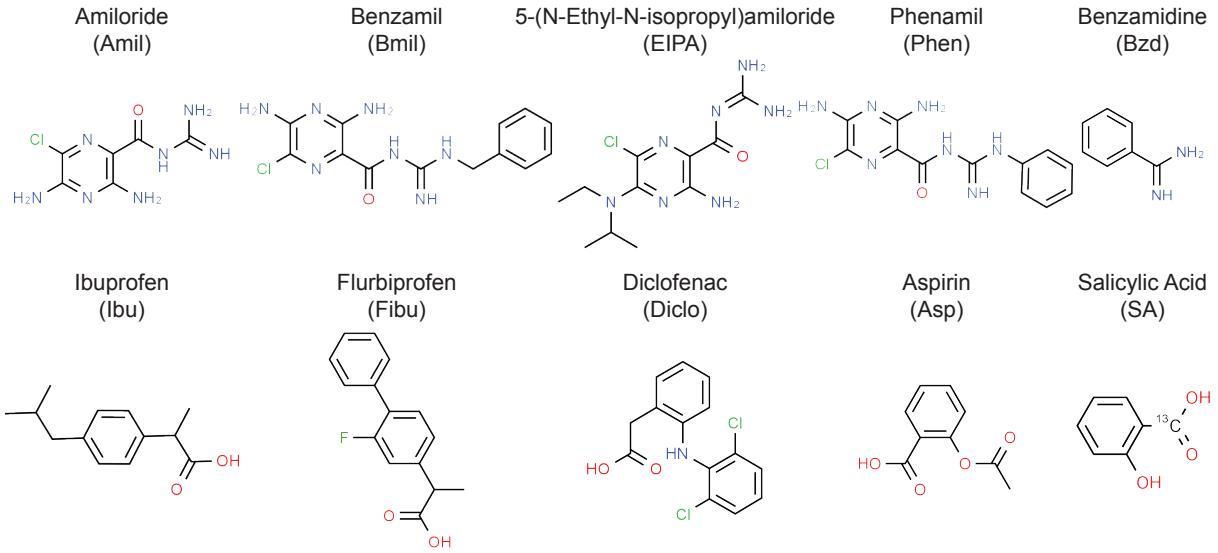


**Figure 3: Chemical structures of amiloride analogs and NSAIDs used in this study.** Chemical structures downloaded from chem spider http://www.chemspider.com/Chemical-Structure.1906.html.

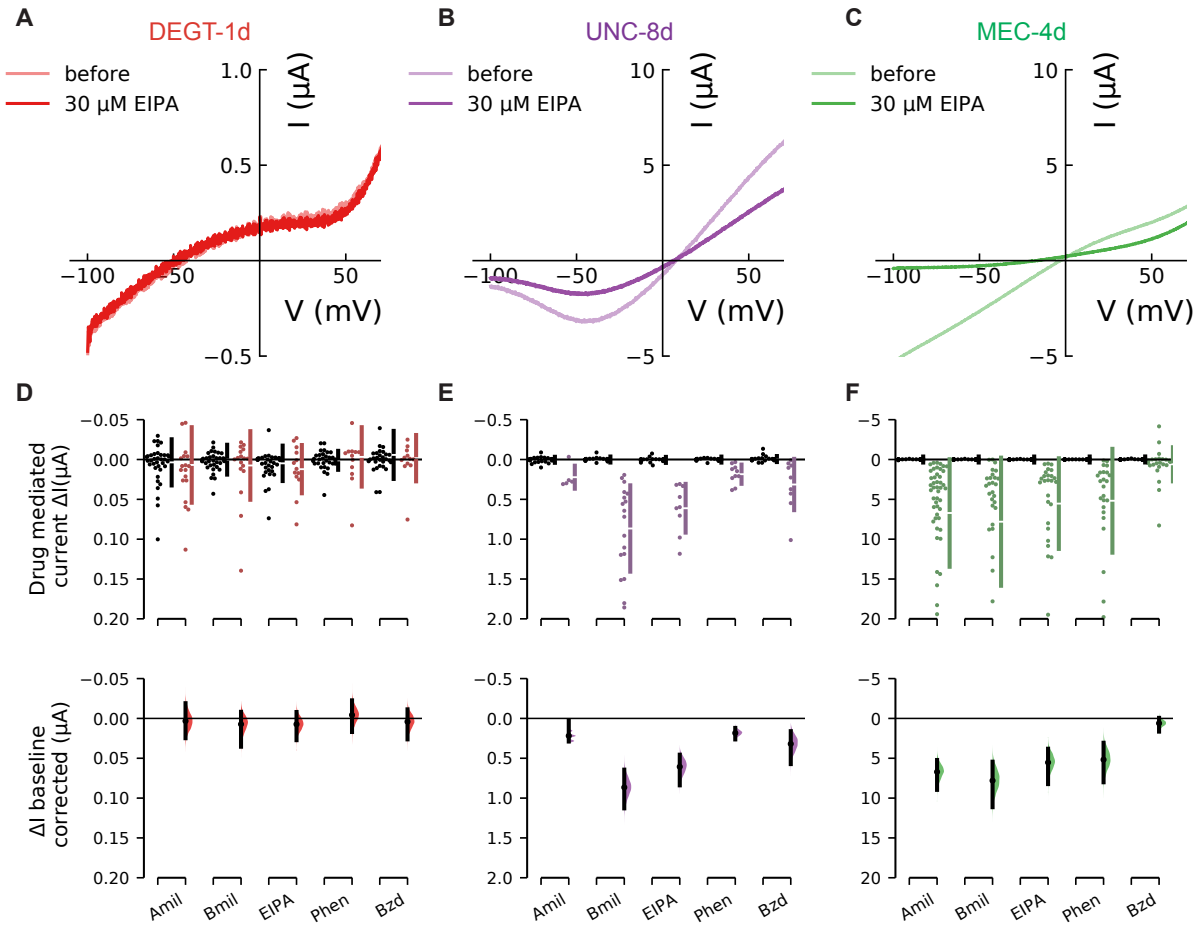


**FIG 4**

**Figure 4: Unlike MEC-4d and UNC-8d, DEGT-1d currents are insensitive to amiloride analogs. A-C:** IV curves of oocytes expressing DEGT-1d (**A**), UNC-8d (**B**) or MEC-4d (**C**) in the presence (darker color) and absence (lighter color) of 30 μM 5-(N-Ethyl-N-isopropyl) amiloride (EIPA) added to control saline. IV curves were derived from the ramp protocol depicted in Fig 1A. **D-F:** Estimation plots to the change in current at -85 mV of oocytes expressing DEGT-1d (**D**), UNC-8d (**E**) or MEC-4d (**F**) (in color) in the presence and absence of 30 μM amiloride (Amil), benzamil (Bmil), EIPA, phenamil (Phen) or benzamidine (Bzd) compared to uninjected oocytes (black). Upper panel: Change in current before (I) and after (Idrug) drug application (uninjected oocytes in black, injected in color). Lower panel: Change in current of oocytes expressing DEGT-1d (**D**), UNC-8d (**E**) or MEC-4d (**F**) subtracted from the change in current of uninjected oocytes. Estimation statistics are given in Table 3-5.

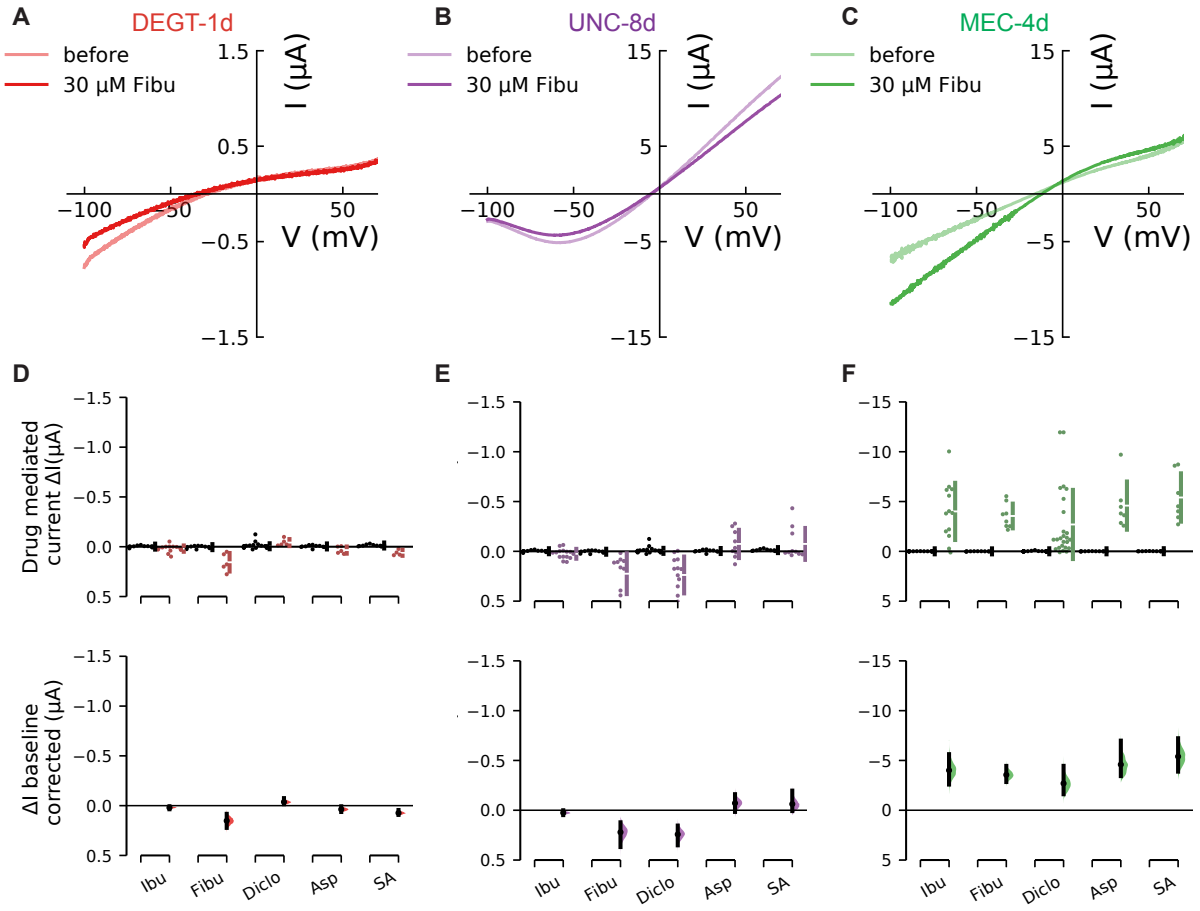


**FIG 5**

**Figure 5: Nonsteroidal anti-inflammatory drugs (NSAIDS) potentiate MEC-4d current and inhibit or are ineffective on DEGT-1d and UNC-8d. A-C:** IV curves of oocytes expressing DEGT-1d (**A**), UNC-8d (**B**) or MEC-4d (**C**) in the presence (darker color) and absence (lighter color) of 30 µM Flurbiprofen (Fibu) added to control saline. IV curves were derived from the ramp protocol depicted in Fig 1A. **D-F:** Estimation plots to the change in current at -85 mV of oocytes expressing DEGT-1d (**D**), UNC-8d (**E**) or MEC-4d (**F**) (in color) in the presence and absence of 30 µM ibuprofen (Ibu), Flurbiprofen (Fibu), Diclofenac (Diclo), Aspirin (Asp), salicylic acid (SA) compared to uninjected oocytes (black). Upper panel: Change in current before (I) and after (Idrug) drug application (uninjected oocytes in black, injected in color). Lower panel: Change in current of oocytes expressing DEGT-1d (**D**), UNC-8d (**E**) or MEC-4d (**F**) subtracted from the change in current of uninjected oocytes. Estimation statistics are given in Table 3-5.

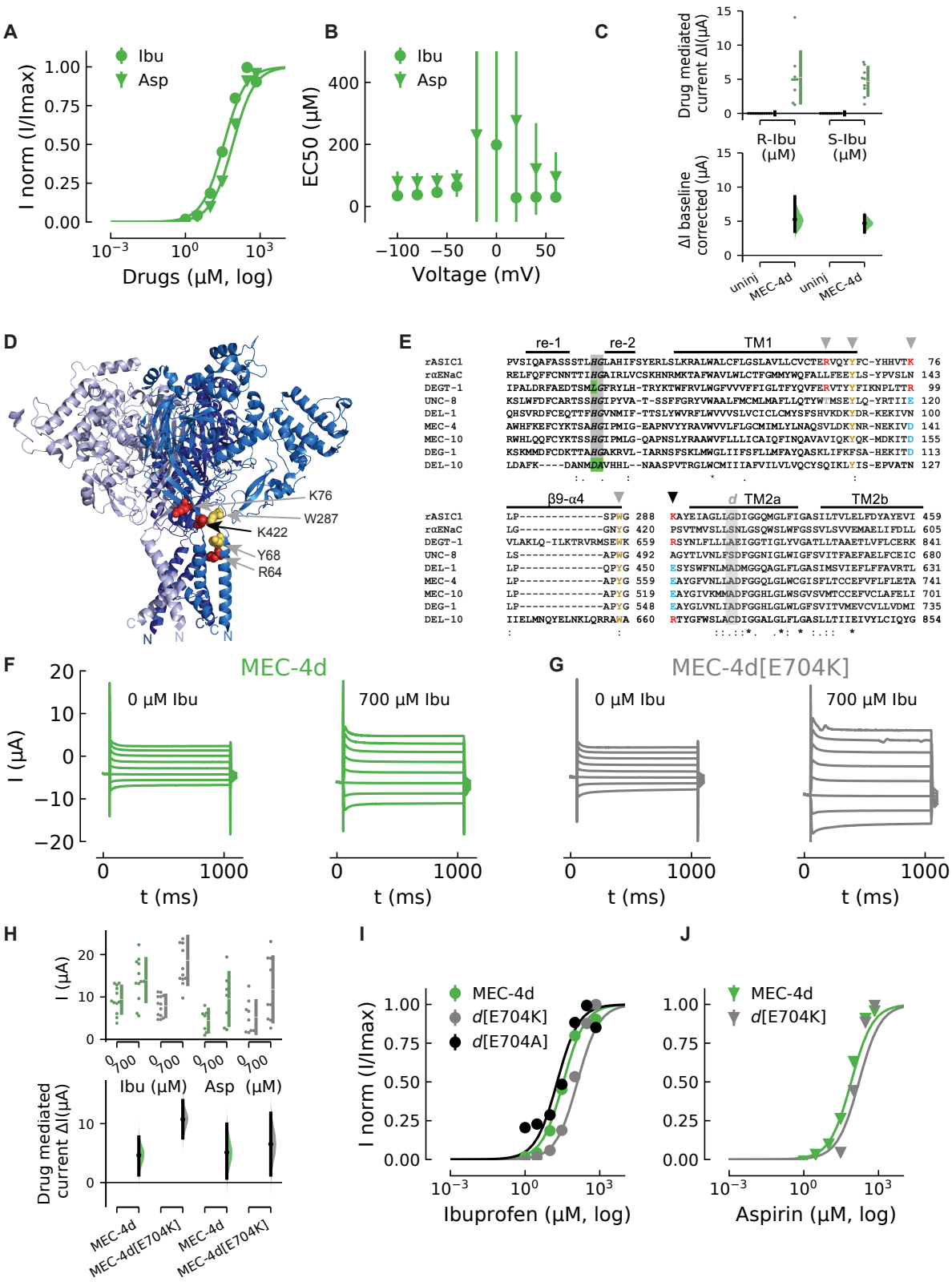
A
Ibu
Asp
I norm (I/Imax)
Drugs (μM, log)
B
Ibu
Asp
EC50 (μM)
Voltage (mV)
C
Drug mediated current ΔI(μA)
R-Ibu (μM)
S-Ibu (μM)
ΔI baseline corrected (μA)
uninj
MEC-4d
D
K76
W287
K422
Y68
R64
E
re-1
re-2
TM1
rASIC1
rαENaC
DEGT-1
UNC-8
DEL-1
MEC-4
MEC-10
DEG-1
DEL-10
β9-α4
d TM2a
TM2b
F
MEC-4d
0 μM Ibu
700 μM Ibu
I (μA)
t (ms)
G
MEC-4d[E704K]
0 μM Ibu
700 μM Ibu
t (ms)
H
I (μA)
Ibu (μM)
Asp (μM)
Drug mediated current ΔI(μA)
MEC-4d
MEC-4d[E704K]
I
MEC-4d
d[E704K]
d[E704A]
I norm (I/Imax)
Ibuprofen (μM, log)
J
MEC-4d
d[E704K]
Aspirin (μM, log)

**FIG 6**

**Figure 6: Amino acid in the wrist close to TM2 in MEC-4d changes sensitivity to ibuprofen and aspirin. A:** Dose-responses curves of oocytes expressing MEC-4d for Ibuprofen (Ibu) (circle) and Aspirin (Asp) (triangle) at -100 mV normalized to $I_{max}$ and baseline current. **B:** $EC_{50}$ values for different voltages for Ibu (circle) and Asp (triangle). **C:** Estimation plots of the change in current at -85 mV (voltage protocol Fig. 1A) of oocytes expressing MEC-4d (green) in the presence and absence of 30 µM R-Ibu and S-Ibu added to control saline compared to uninjected oocytes (black). Upper panel: Change in current before (I) and after (Idrug) drug application. Lower panel: Change in current of occytes expressing MEC-4d subtracted from the change in current of uninjected oocytes. Estimation statistics are given as the 95% confidence interval [in µA], and the two-sided p-value of the Mann-Whitney test. The difference for MEC-4d for 30 µM R-Ibu is 5.27 µA [3.49, 8.62], p = 0.000197 and for 30 µM S-Ibu is 4.7 µA [3.39, 5.91], p = 0.00028. **D:** Ribbon diagram of trimeric cASIC1a based on pdb 4NTW made in PyMOL. Highlighted are amino acids identified to impact Ibu binding in rASIC1a (Lynagh et al., 2017b). **E:** Amino acid alignment of rASIC1, rαENaC, DEGT-1, UNC-8, MEC-4, DEL-1, MEC-10, DEG-1 and DEL-10 made with Clustal Omega. Only amino acids around transmembrane domain 1 (TM1), a region around ß9-α4 and TM2 are depicted. Black Arrowhead indicates rASIC1a[K422], an amino acid position involved in Ibu sensitivity. The grey *d* indicates the degeneration site. Amino acids discussed in Ibu sensitivity in rASIC1 highlighted in colors: red (positively charged), blue (negatively charged) and yellow (hydrophobic). The HG motif in the N-terminal region is highlighted in dark grey. Those differing from the HG motif are highlighted in green. **F-G:** Current traces of oocytes expressing MEC-4d (**F**) or MEC-4d[E704K] (**G**) channels in the absence 0 (left) or presence of 700 µM (right) ibuprofen (Ibu) added to control saline. **H:** Estimation plots to the change in current at -85 mV (voltage protocol Fig. 1A) of oocytes expressing MEC-4d (green) or MEC-4d[E704K] (grey) in the presence of 700 µM Ibu or aspirin (Asp) compared to the absence of the drugs. Upper panel: Current (I) in the presence and absence of a drug. Lower panel: Current of oocytes expressing MEC-4d superfused with Ibu or Asp subtracted from the current before drug application. Estimation statistics are given as the 95% confidence interval [in µA], and the two-sided p-value of the Mann-Whitney test. The difference of 0 µM and 700 µM Ibu for MEC-4d is 4.63 µA [1.29, 7.73], p = 0.0102 (n = 12) and for MEC-4d-E704K 10.7 µA [7.58, 13.9], p = 5.09e-05 (n = 13). The difference of 0 µM and 700 µM Asp for MEC-4d is 5.11 µA [0.74, 9.92], p = 0.073 (n = 7) and for MEC-4d[E704K] 6.53 µA [1.28, 11.8], p = 0.0521 (n = 9). **I:** Dose-responses

curves of oocytes expressing MEC-4d (green), MEC-4d[E704K] (grey) and MEC-4d[E704A] (black) for Ibu at -100 mV normalized to Imax and baseline current. **J:** Dose-responses curves of oocytes expressing MEC-4d (green) and MEC-4d-E704K (grey) for Asp at -100 mV normalized to $I_{max}$ and baseline current. Mean values for dose-response curves were derived from a step protocol similar to Fig 1A. Instead of the ramp (red background), voltage steps from -100 mV to +40 mV in 20 mV increments were applied. Individual recordings were fitted with the Hill equation ($I_{max}$* $IC_{50}^{n}$/ ($IC_{50}^{n}$ +$x^{n}$)), where the Hill parameter was set to 1 and x is the concentration of the drug.

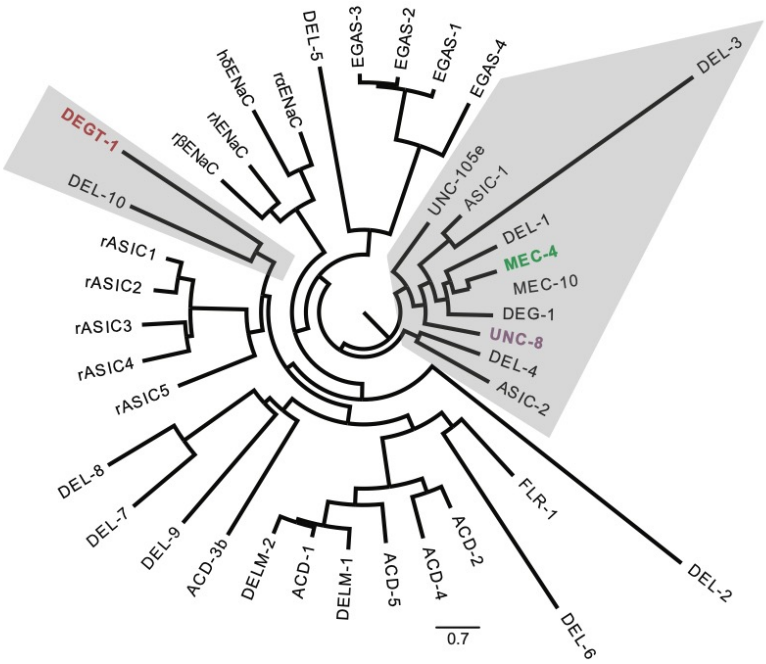


**Figure 7: Phylogenetic tree of the 30 C. elegans DEG/ENaC/ASIC subunits compared to mammalian ENaC and ASIC subunits.** Accession numbers are given in material and methods.

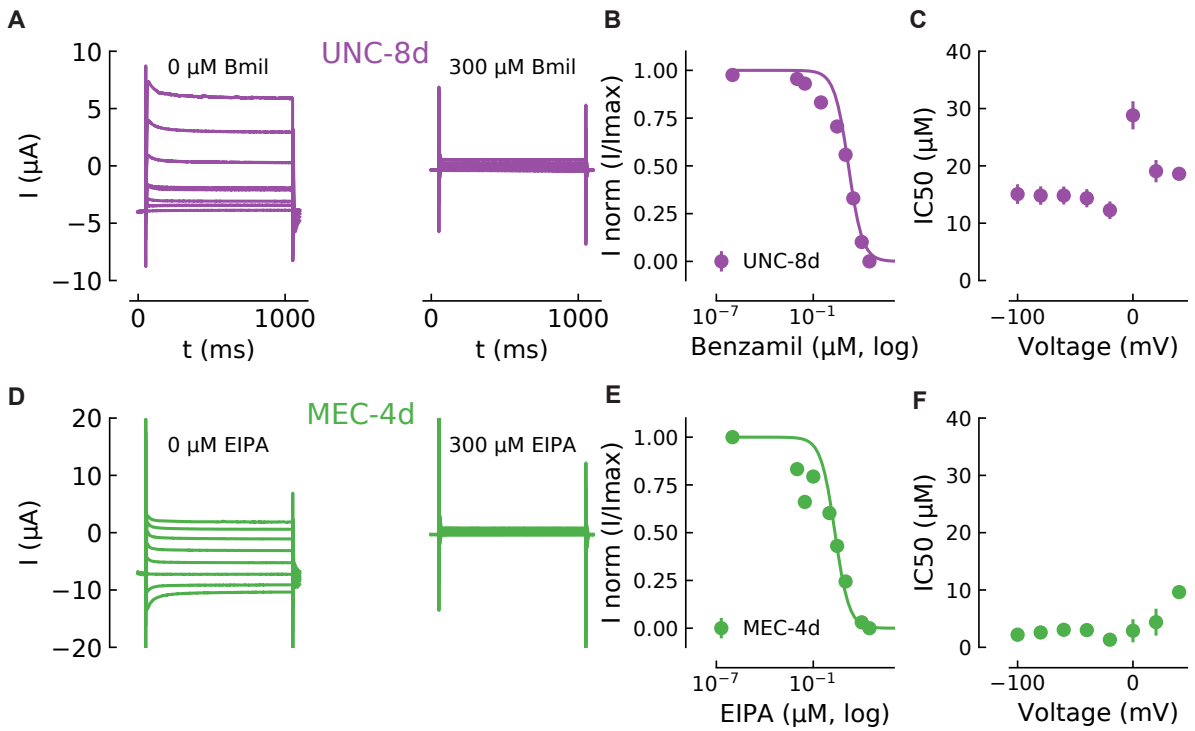


**Supplementary-Figure 1: Sensitivity of UNC-8d channels to Benzamil and MEC-4d channels to EIPA. A:** Representative traces of currents of oocytes expressing UNC-8d channels in the absence (left) and presence (right) of 300 µM Benzamil (Bmil). Current responses to voltage steps from -100 mV to +40 mV in 20 mV increments. **B:** Dose-response curves of UNC-8d channels to Bmil at -60 mV. The mean $IC_{50}$ ± SEM for Bmil at -60 mV was 14.8 ± 1.6 µM (n = 4). **C:** $IC_{50}$ values for different voltages (n = 4). **D:** Representative traces of currents of oocytes expressing MEC-4d channels in the absence (left) and presence (right) of 300 µM 5-(N-Ethyl-N-isopropyl) amiloride (EIPA) added to control saline. Current responses to voltage steps from protocol depicted in Fig 2A from -100 to +40 mV. **E:** Dose-response curves of oocytes expressing MEC-4d channels exposed to EIPA at -60 mV normalized to Imax and baseline current. The mean $IC_{50}$ ± SEM for EIPA at -60 mV was 3.1 ± 0.1 µM (n = 11). **F:** $IC_{50}$ values for different voltages (n = 11, except 0 + 20 mV n=2 and +40 mV n =1). Mean values for dose-response curves were derived from the step protocol (ii) depicted in Fig 2A. Individual recordings were fitted with the Hill equation ($I_{max} * {IC_{50}}^n/({IC_{50}}^n + x^n)$), where the Hill parameter was set to 1 and x is the concentration of the drug.